SAND REPORT

SAND2001-3611
Unlimited Release
Printed November 2001

Rio Grande Erosion Potential Demonstration Report for the National Border Technology Partnership Program

Rich Jepsen, Jesse Roberts, Richard Langford, Joseph Gailani

Prepared by
Sandia National Laboratories
Albuquerque, New Mexico 87185 and Livermore, California 94550

Sandia is a multiprogram laboratory operated by Sandia Corporation, a Lockheed Martin Company, for the United States Department of Energy under Contract DE-AC04-94AL85000.

Issued by Sandia National Laboratories, operated for the United States Department of Energy by Sandia Corporation.

Available to DOE and DOE contractors from
U.S. Department of Energy
Office of Scientific and Technical Information
P.O. Box 62
Oak Ridge, TN 37831

Telephone: (865)576-8401
Facsimile: (865)576-5728
E-Mail: reports@adonis.osti.gov
Online ordering: http://www.doe.gov/bridge

Available to the public from
U.S. Department of Commerce
National Technical Information Service
5285 Port Royal Rd
Springfield, VA 22161

Telephone: (800)553-6847
Facsimile: (703)605-6900
E-Mail: orders@ntis.fedworld.gov
Online order: http://www.ntis.gov/ordering.htm

SAND 2001-3611
Unlimited Release
Printed November, 2001

Rio Grande Erosion Potential Demonstration

Report for the National Border Technology Partnership Program

Rich Jepsen and Jesse Roberts
Carlsbad Programs Group
Soil and Sediment Transport Lab
Sandia National Laboratories
P.O. Box 5800
Albuquerque, NM 87185-1395

Richard Langford
University of Texas, El Paso
El Paso, Texas

Joseph Gailani
U.S. Army Corps of Engineers
Coastal and Hydraulics Laboratory
Vicksburg, MS 39180

Abstract

This demonstration project is a collaboration among DOE, Sandia National Laboratories, the University of Texas, El Paso (UTEP), the International Boundary and Water Commission (IBWC), and the US Army Corps of Engineers (USACE). Sandia deployed and demonstrated a field measurement technology that enables the determination of erosion and transport potential of sediments in the Rio Grande. The technology deployed was the Mobile High Shear Stress Flume. This unique device was developed by Sandia's Carlsbad Programs for the USACE and has been used extensively in collaborative efforts on near shore and river systems throughout the United States. Since surface water quantity and quality along with human health is an important part of the National Border Technology Program, technologies that aid in characterizing, managing, and protecting this valuable resource from possible contamination sources is imperative.

Acknowledgements

The authors would like to thank the following people for there efforts in coordinating and supporting the field and laboratory work for this project.

Bill Halford, USACE

Gabriel Chavez, SNL

Manuel Rubio, Jr., IBWC

Rong Kuo, IBWC

Octavio Anchondo, UTEP

Wildaliz deJesus, UTEP

Yaysa Sanchez, UTEP

TABLE OF CONTENTS

LIST OF TABLES

LIST OF FIGURES

1. Introduction

This demonstration project is a collaboration among DOE, Sandia National Laboratories, the University of Texas, El Paso (UTEP), the International Boundary and Water Commission (IBWC), and the US Army Corps of Engineers (USACE). Sandia deployed and demonstrated a field measurement technology that enables the determination of erosion and transport potential of sediments in the Rio Grande. This unique technology was developed by Sandia's Carlsbad Programs Group for the USACE and has been used extensively in collaborative efforts on near shore and river systems throughout the United States. Since surface water quality and human health is an important part of the National Border Technology Program, application of technologies that aid in characterizing, managing, and protecting this valuable resource from possible contamination sources is imperative. This demonstration proved that the transfer of the flume technology to a border agency would be very helpful in determining sediment-water interactions and their effects on water quality and management as it relates to public health and economic development.

The technology deployed was the Mobile High Shear Stress Flume. This device measures in-situ sediment erosion properties at shear stresses ranging from normal flow to flood conditions for a variable depth sediment core. It is housed in a self-sufficient trailer that can be placed on site in the field. The data derived from these tests characterize the erosion potential of the sediments of concern allowing for management decisions directly from the data or by incorporation into a model.

The El Paso Valley was used as a demonstration site because it has been heavily stressed by development and population pressures along the border and because it has been cited as an area of key environmental and public health concern by the U.S. – Mexico field coordinating

committee. The demonstration study focused on the stretch of the Rio Grande between El Paso and Fort Quitman, Texas, in the southern end of the engineered channel of the Rio Grande. Three field study sites were selected. The first was at the Riverside Dam, the second was at Alamo Arroyo, and the third was at Balluco Arroyo. A study at the first site looked at potential erosion of sediments that were deposited behind the dam prior to its destruction in a flood in 1987. These sediments may be potentially remobilized by subsequent flooding. The second and third sites are where large arroyos enter the Rio Grande from the American side. These arroyos provide periodic influxes of sediment that obstruct the channel from the Rio Grande and may cause channel overflow as well as sedimentation problems farther downstream. Each site was mapped and characterized in terms of vegetation and soil distribution. Sediment samples were collected and erosion rates and sediment grain size distributions were determined.

2. Experimental Procedures

2.1 Description of the Mobile High Shear Stress Flume

The High Shear Stress Sediment Erosion Flume is shown in Figure 2.1a and is essentially a straight flume, which has a test section with an open bottom through which a rectangular cross-section coring tube containing sediment can be inserted. The main components of the flume are the coring tube; the test section; an inlet section for uniform, fully-developed, turbulent flow; a flow exit section; a water storage tank; and a pump to force water through the system. The coring tube, test section, inlet section, and exit section are made of clear acrylic or polycarbonate so that the sediment-water interactions can be observed. The coring tube can be rectangular with a 10 by 15 cm cross-section or circular with a 10 cm diameter. The length can be up to 1 m.

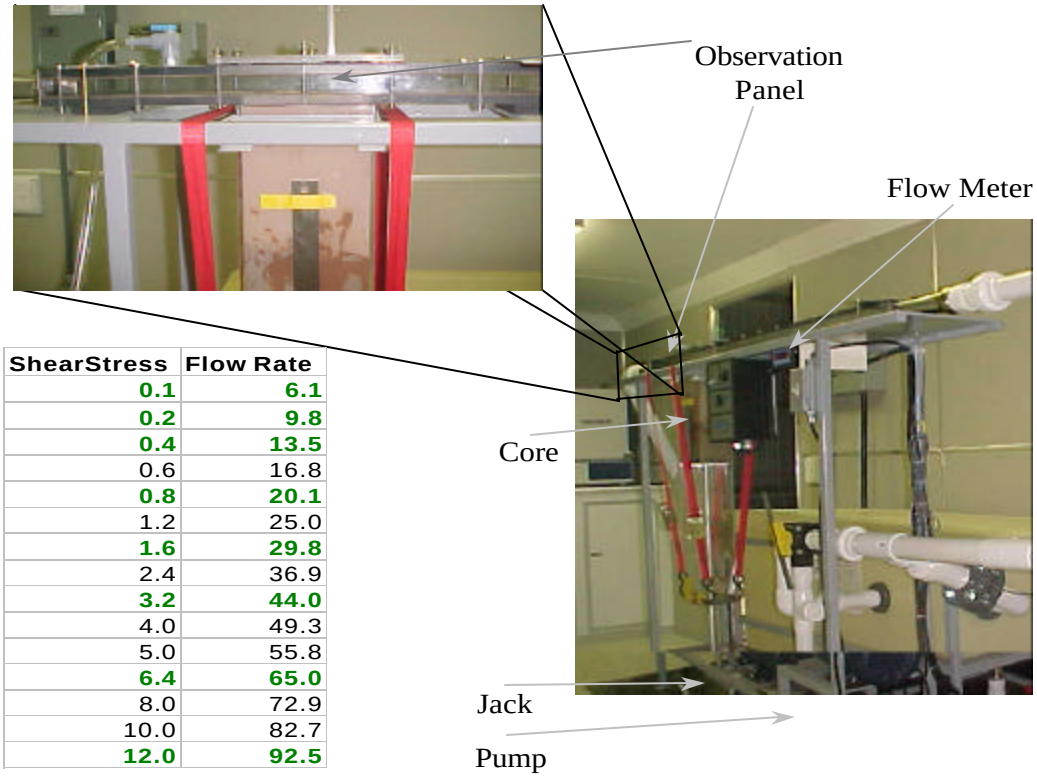

ShearStress	Flow Rate
0.1	6.1
0.2	9.8
0.4	13.5
0.6	16.8
0.8	20.1
1.2	25.0
1.6	29.8
2.4	36.9
3.2	44.0
4.0	49.3
5.0	55.8
6.4	65.0
8.0	72.9
10.0	82.7
12.0	92.5

Figure 2.1a. Mobile High Shear Stress Flume illustration

The flume is housed in a 20 ft mobile trailer (Figure 2.1b) so it can be easily moved to each site of interest. The trailer is self-contained with a gas generator for electric power and pumps for water intake from external sources.

Figure 2.1b Mobile Flume at Riverside Dam

Water is pumped through the system from a 120-gallon storage tank, through a 5 cm diameter pipe, and then through a flow converter into the rectangular duct shown. This duct is 2.5 cm in height, 10 cm in width, and 100 cm in length; it connects to the test section, which has the same cross-sectional area and is 15 cm long (see Figure 2.1a, observation panel). The flow converter changes the shape of the cross-section from circular to the rectangular duct. The flow is regulated by a three-way valve so that part of the flow goes into the duct while the remainder returns to the tank. Also, there is a small valve in the duct immediately downstream from the test section, which is opened at higher flow rates to keep the pressure in the duct and over the test section at atmospheric conditions.

Cores can either be taken in-situ from the field or reconstructed in the laboratory. The procedure for preparing the reconstructed sediments in the laboratory will be described later. The coring tube and the sediment it contains are then inserted into the bottom of the test section. An operator moves the sediment upward using a piston, which is inside the coring tube and is connected to a mechanical jack and then driven by a variable-speed controller. By this means, the sediments can be raised and made level with the bottom of the test section by a trained operator. The speed of the jack movement can be controlled at a variable rate in measurable increments as small as 0.25 mm.

Water is forced through the duct and the test section over the surface of the sediments. The shear produced by this flow causes the sediments to erode. As the sediments in the core erode, they are continually moved upwards by the operator so that the sediment-water interface remains level with the bottom of the test and inlet sections. The erosion rate is recorded as the upward movement of the sediments in the coring tube over time.

2.2 Hydrodynamics

For the flow rates of interest, it can be shown that fully developed turbulent flow exists in the test section. Turbulent flow through pipes has been studied extensively, and empirical functions have been developed which relate the mean flow rate to the wall shear stress. In general, flow in circular cross-section pipes has been investigated. However, the relations developed for flow through circular pipes can be extended to non-circular cross-sections by means of a shape factor. An implicit formula relating the wall shear stress to the mean flow in a pipe of arbitrary cross-section can be obtained from Prandtl's Universal Law of Friction (Schlichting, 1979). For a pipe with a smooth surface, this formula is

$$\frac{1}{\sqrt{l}} = 2.0 \log\left[\frac{UD\sqrt{l}}{n}\right] - 0.8 \qquad (2.1)$$

where U is the mean flow speed, ν is the kinematic viscosity, λ is the friction factor, and D is the hydraulic diameter defined as the ratio of four times the cross-sectional area to the wetted perimeter. For a pipe with a rectangular cross-section, or duct, the hydraulic diameter is

$$D = 2hw/(h + w) \qquad (2.2)$$

where w is the duct width and h is the duct height. The friction factor is defined by

$$l = \frac{8t}{r\mathrm{U}^2} \qquad (2.3)$$

where ρ is the density of water and τ is the wall shear stress. Inserting Eqs. (2.2) and (2.3) into Eq. (2.1) then gives the wall shear stress τ as an implicit function of the mean flow speed U.

For shear stresses in the range of 0.1 to 10 N/m^2, the Reynolds numbers, UD/ν, are on the order of 10^4 to 10^5. These values for Reynolds numbers are sufficient for turbulent flow to exist for the stresses of interest in this study. For flow in a circular pipe, turbulent flow theory suggests that the transition from laminar to turbulent flow occurs within 25 to 40 diameters from the entrance to the pipe. Since the hydraulic diameter of the duct pipe is 4.0 cm, this suggests an entry length of approximately 100 cm. The length of the duct leading to the test section is 100 cm and is preceded by a 20 cm flow converter and several meters of inlet pipe. These arguments along with direct observations indicate that the flow is fully turbulent in the test section.

2.3 Core Retrieval

Cores were obtained in situ by applying pressure to the top of the core sleeve and, penetrating into the sediment bed (Figure 2.3). The coring sleeve is then pushed as far as possible into the sediment bed; the distance of penetration will vary due to the characteristics of the sediment (i.e., further penetration will occur in a softer sediment than in a more compact sediment). This results in a sediment core that is obtained relatively undisturbed from its natural surroundings. The coring sleeve is then brought back and a plug is slid up into the core tube to act later as a piston, and the core is then capped. Sediment cores varying in length from 10 to 30 cm were obtained by this method.

Figure 2.3. Sediment sampling at Alamo Arroyo and Riverside Dam

Sediments from Balluco Arroyo were gathered into 5 gallon buckets with a shovel and taken back to the laboratory. This was done because of time and funding constraints on the project limited the opportunity to obtain in-situ cores as described above. These sediments were generally non-cohesive sands and were mixed with water and placed into the same erosion cores used in the field. The cores were made such that the sediment depth in them was 30 cm. Full

description of this procedure can be found in Jepsen et al, 2001 and Roberts et al, 1998 and 2001b.

2.4 Measurements of Sediment Erosion Rates

The procedure for measuring the erosion rates of the sediments in circular cores (Roberts et al, 2001a) as a function of shear stress and depth was as follows. The sediment cores were prepared as described above and then moved upward into the test section until the sediment surface was even with the bottom of the test section. A measurement was made of the depth to the bottom of the sediment in the core. The flume was then run at a specific flow rate corresponding to a particular shear stress. Erosion rates were obtained by measuring the remaining core length at different time intervals, taking the difference between each successive measurement, and dividing by the time interval.

In order to measure erosion rates at several different shear stresses using only one core, the following procedure was generally used. Starting at a low shear stress, the flume was run sequentially at higher shear stresses with each succeeding shear stress being twice the previous one. Generally about three shear stresses were run sequentially. Each shear stress was run until at least 1 to 3 mm but no more than 2 cm were eroded. Also, each shear stress was run for a minimum of 20 seconds and a maximum of 10 minutes. This defines the minimum and maximum erosion rates measured by the high shear stress sediment erosion flume to be 1.67×10^{-4} and 0.1 cm/s respectively. The time interval was recorded for each run with a stop watch. The flow was then increased to the next shear stress, and so on until the highest shear stress was run. This cycle was repeated until all of the sediment had eroded from the core. If after three cycles a particular shear stress showed a rate of erosion less than approximately 1.7×10^{-4} cm/s,

it was dropped from the cycle; if after many cycles the erosion rates decreased significantly, a higher shear stress was included in the cycle.

2.5 Measurements of Critical Shear Stress for Erosion

A critical shear stress can be quantitatively defined as the shear stress at which a very small, but accurately measurable, rate of erosion occurs. In the present study, this rate of erosion was chosen to be 1.7×10^{-4} cm/s; this represents 1 mm of erosion in approximately 10 minutes.

2.6 Measurements of Sediment Bulk Properties

Particle sizes and particle size distributions were determined by use of a Malvern Mastersizer S particle sizing package for particle diameters between 0.05 and 900 μm. Sieve analysis was done for particle sizes larger than 900 μm. When using the Malvern particle sizer, approximately 5 to 10 grams of sediment was placed in a beaker containing about 500 mL of water and mixed by means of a magnetic stir bar/plate combination. Approximately 1 mL of this solution was then inserted into the sizers sampling system and further disaggregated as it is re-circulated through the sampling system by means of a centrifugal pump. The sample was allowed to disaggregate for five minutes on the stir plate and an additional five minutes in the recirculating pump sampling system before analysis by the sizer. To ensure complete dissagregation and sample uniformity the sediment samples were analyzed multiple times and repeated in triplicate. From these measurements, the distribution of grain sizes and mean grain sizes as a function of depth were obtained.

2.7 Topography

Topography was measured at each site in order to provide a three-dimensional characterization of the site. The detailed topographic maps provide accurate locations for the samples collected for erosion analysis and allowed inferences to be made about how representative those samples are. Topographic maps are also useful for identifying geomorphic changes that might be associated with changes in sediment character. Topography was measured using a survey-quality Trimble 3100 global positioning system. A kinematic survey was performed that gives the precision of approximately 2 cm in latitude and longitude and approximately 5 cm in elevation. GPS points were collected along the edges of topographic features so that they also defined the edges of channels and terraces, in addition to providing elevations. Data points are provided in appendix A.

The topographic maps illustrate the geomorphic features at each site. Geomorphic features present at all sites include the river channels, constructional terraces and, man-made levees. Levees are the highest topographic features, and have been constructed approximately 1.5 m above the surrounding flood plain. The levees sit on the Rio Grande flood plain, which lies 50 cm to 2 m above the channel. Inset into the flood plain are younger construction terraces formed by floods of the Rio Grande. The youngest of these terraces lies only 30 to 50 cm above the stream water level and exhibits evidence of recent floods. Higher terraces can be found 50 cm to 1 m above these low terraces. The discharge in the Rio Grande Channel during the study period was 3.5 m^3/s at Fort Quitman, which is similar to Alamo Arroyo and Balluco Arroyo. The channel under these conditions was approximately 50 cm deep and 15-20 meters wide with flow velocities of approximately 0.4 m/sec. At Riverside dam the channel was over 2 m deep and contained stagnant water.

2.8 Electromagnetic Conductivity

The electromagnetic conductivity was measured using a Geonics Ltd. EM-31 ground conductivity meter (McNiel, 1992). The ground conductivity meter measures an apparent conductivity of the sediment below it, based on the assumption that the sediment is homogenous. The EM-31 provides apparent conductivities to 3 m deep in the horizontal mode, and to 6 m deep in the vertical mode. EM-31 device works by generating an electrical current in one end of the device. This current generates a magnetic field that in turn, generates electrical fields in the earth. The EM-31 receiver detects the magnitude of these electric currents and provides the user with an apparent conductivity in MilliSiemens per meter (mS/m). The EM-31 measures conductivities in both quadraphase and in-phase modes. In-phase conductivities respond best to buried metal objects, pipelines, and other artificial features. Quadraphase conductivity responds to changes in sediment salinity, grain size, and water content. Maps of apparent conductivity were prepared from spatially distributed the EM-31 measurements at Riverside dam and Alamo Arroyo. Conductivities were not measured at Balluco Arroyo because the Arroyo channel was under water during our investigation. The most useful conductivity maps were the quadraphase conductivities measured in horizontal mode, which responds best to changes in sediment parameters in the shallow that we studied for erosion. These maps are presented in this report. EM conductivity data, along with the measurement locations is provided in appendix B.

3. Results

In order to describe two separate problems, the results will individually present the Riverside Basin and the Arroyo effects on the Rio Grande. Appendix C gives all particle distributions for each sample site and depth in each core.

3.1 Riverside Flood Basin

The Riverside Flood Basin was divided into two sections: the channel with its associated flood plain and then the levee that banks the north (American) side of the basin.

3.1.1 Channel and Flood Plain

3.1.1a Morphology

The Riverside flood basin is north of Riverside dam at the southeastern edge of the city of El Paso. The Riverside dam was constructed to allow diversion of water from the Rio Grande into the Riverside Canal. In 1987, releases of water from Caballo Reservoir caused a flood that severely damaged the Riverside Dam. Following this event the Riverside Canal was extended upstream to a new diversion facility. Today the Riverside Dam does not hold water and the study site was on the sediments that once filled the flood basin behind the dam.

The study site is located approximately 100 m north of the Riverside Dam, just south of the old diversion structure for the Riverside Canal. North of the study area is a large pond that once served as part of the diversion structure to the Riverside canal, which is just north of the study area. The edge of the canal extends southwest for approximately 15 m and then East-West to

where it meets the real grounded channel. The region of study in the Rio Grande channel also follows a North-South trend and follows the western edge of the study area.

Figure 3.1a is a topographic map of the study site that illustrates the four major features present: 1) The levee which is 1.2 m high and extends along the eastern edge of the study area. 2) The historic flood plain of the Rio Grande, which is found between the 1,094 m and the 1,093.4 m contours. The flood plain has been elevated by addition of artificial materials in the northern part of the study area. 3) A lower terrace of flood plain sediments that occurs below the 1093 m contour that contains sediments deposited behind the dam and sediments added by subsequent floods. 4) The channel of the Rio Grande, which was inactive at the time of our study but contained over 2 meters of water that was impounded in the scours behind the Riverside Dam.

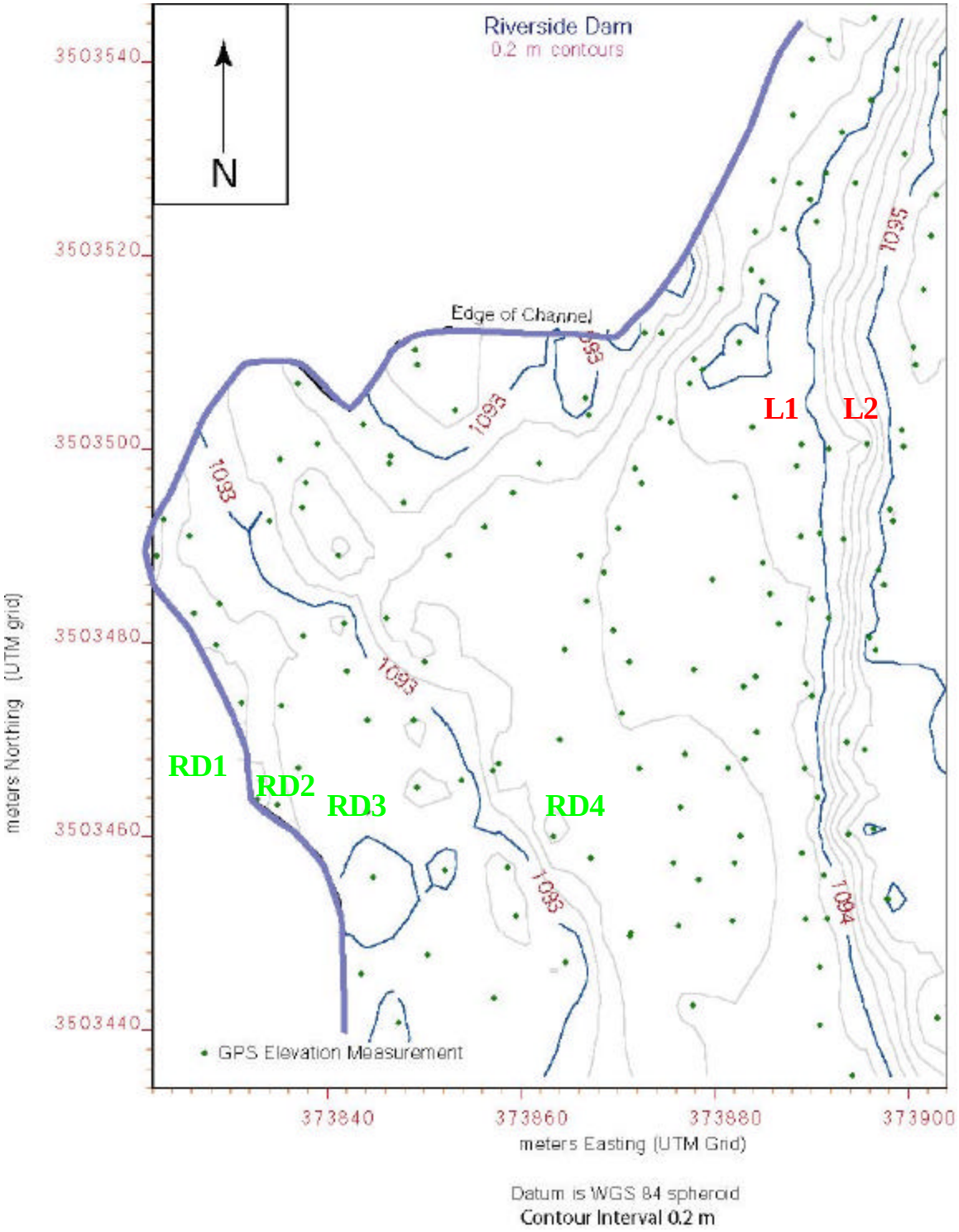

Figure 3.1a. Topographic map of Riverside Dam flood basin with sample locations.

3.1.1b Electromagnetic Conductivity

Figure 3.1b is an EM conductivity map of the Riverside Dam site. Two areas of high conductivity are evident as red, yellow, and green patches on the map. The Levee shows high conductivity, probably due to a high percentage of fines and possibly to metals incorporated into the artificial fill. The historic floodplain shows low conductivities, including the lowest at the study site. This indicates relatively sandy sediment within the top 3 meters. The homogeneity of the flood plain is striking and suggests that this area may lie within an earlier channel fill containing a thick sand. The riverbank also shows low conductivities. Because the water table is near the surface, this indicates fresh water and thick sand-rich sediment. An area of high conductivity is found in the lower terrace and flood plain, just below the historic floodplain. This high conductivity is associated with the edge of the artificial channel across which the Riverside dam was constructed. The high conductivity is due either to a pocket of saline water, or to clays within the subsurface. We will auger some holes to determine which of these factors is present.

The key findings from the EM study are that the samples collected for this experiment are representative of the areas from which they were collected. Samples RD1 and RD2 were collected in the low conductivity sediments in and next to the stream channel. Sample RD4 was collected from the margin of the high-conductivity area in the upper floodplain.

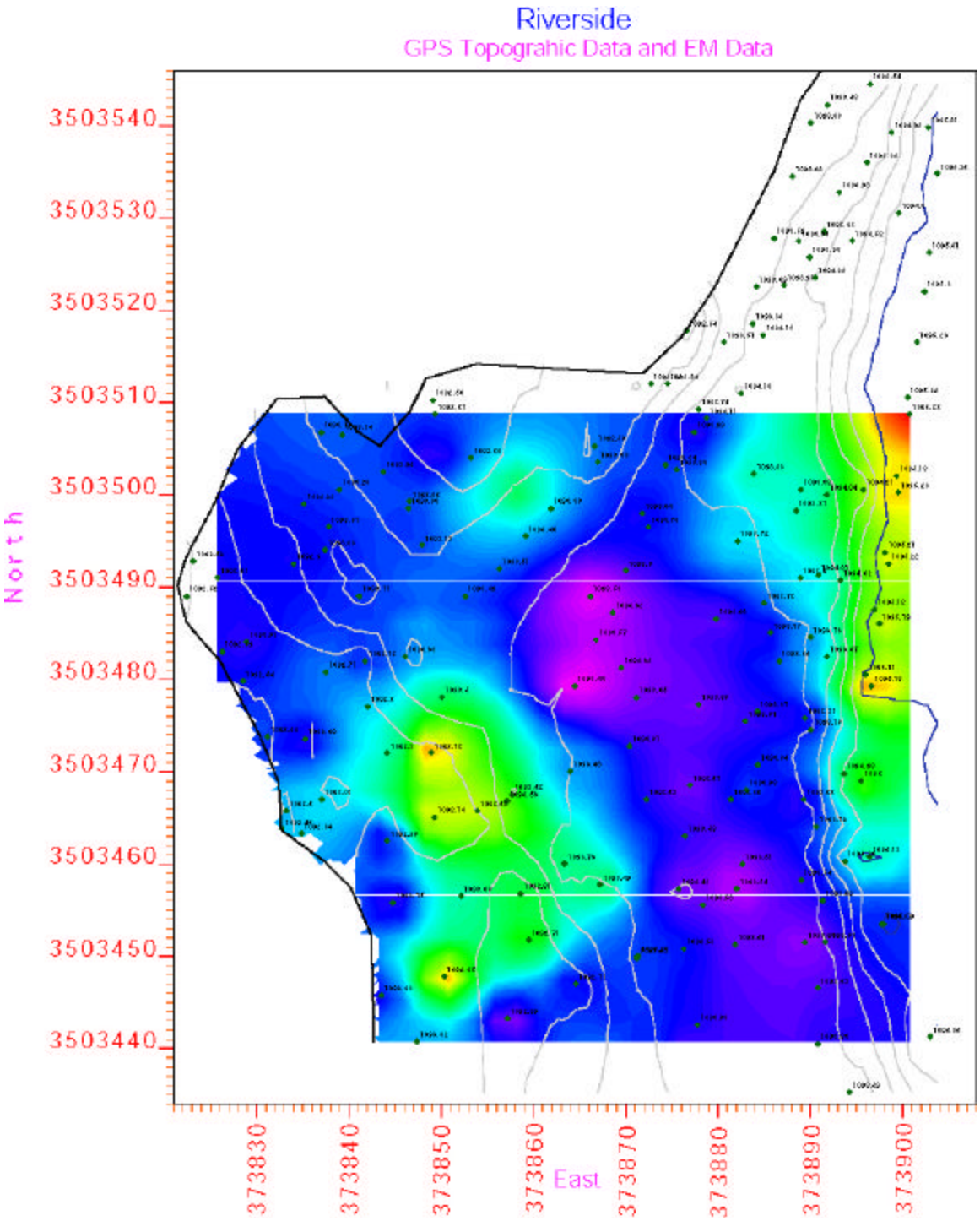

Figure 3.1b. Electromagnetic conductivity map of Riverside Dam flood basin. High conductivities are red and are 130mS/m, Low conductivities are purple and are 78 mS/m.

3.1.1c Erosion Processes

Four cores were retrieved from this area; two in the channel and two from the flood plain. The locations are shown on Figure 3.1a.

The core obtained from the middle of the channel, RD1, was 12 cm in length. The core was observed to contain sand mixed with mud with sand being more prevalent near the surface. The average particle size data shows the same trend in Figure 3.1c.

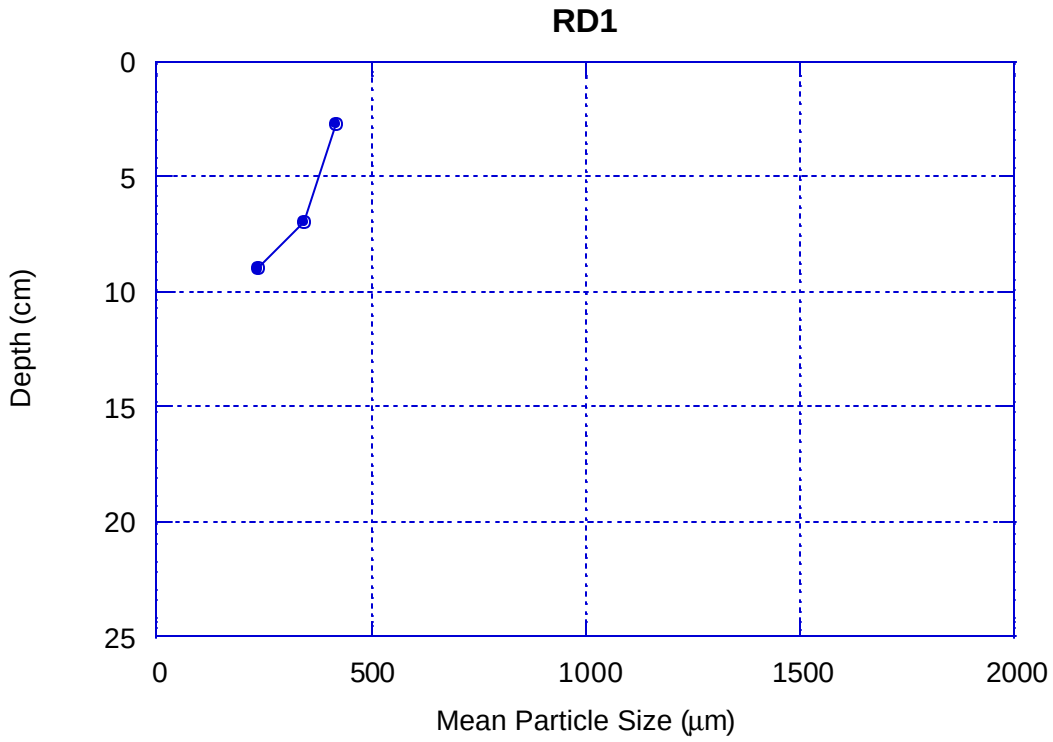

Figure 3.1c

The erosion data as a function of shear stress is shown in Figure 3.1d. For each shear stress, the erosion rate decreased with depth. The sediment was also observed to behave in a more cohesive manner with depth as the mud became more dominant. The critical shear stress was 0.3 Pa in the top 5 cm and 0.4 Pa for the bottom portion of the sample.

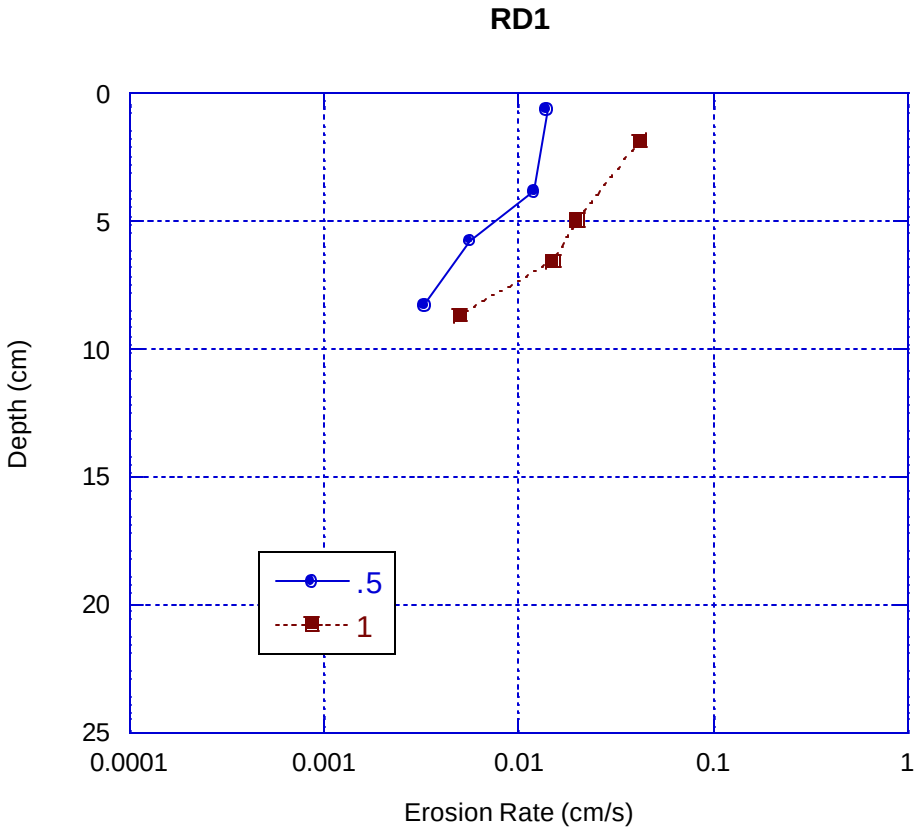

Figure 3.1d

The sample taken at the edge of the channel, RD2, was 19 cm in length. The surface of the sediment had organic debris mixed with sand. The next 4 cm was generally sand and the remainder of the core was observed to contain fine-grained sand and mud (Figure 3.1e). This can be seen visually in Figure 3.1f.

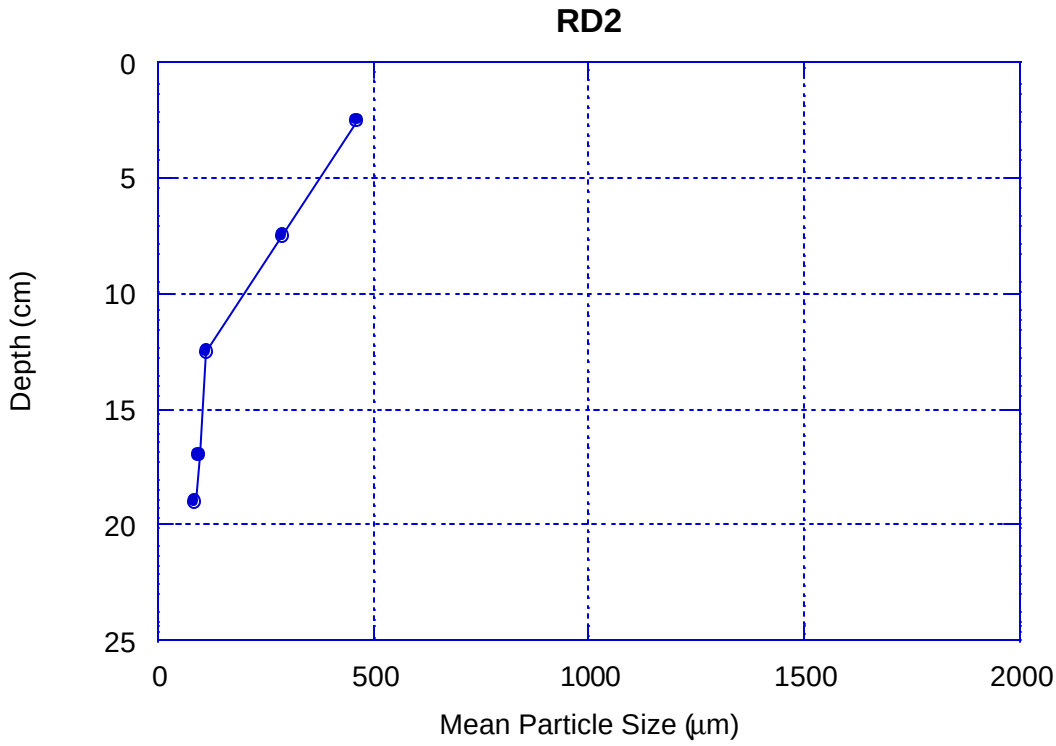

Figure 3.1e

Figure 3.1f. RD2 core samples

The erosion data for RD2 is shown in Figure 3.1g. The top 5 cm had constant erosion rates with depth for both the 0.5 and 1.0 Pa shear stresses. The erosion rates in this region were also very similar to the top portion of the RD1 sample. The transition to the muddy section of the core was very clear. This can be seen in the rapid decrease in erosion rate for 0.5 and 1.0 Pa at 5 to 6 cm of depth and the need to increase the shear stress from 2.0 to 4.0 Pa at subsequent depths. The lower portion of the core displayed much more variability of erosion rates as a function of depth for each shear stress than the top 5 cm layer. There was also some large organic debris such as leaves and plant material that affected the erosion in this region. However, the general trend was a decrease in erosion rate with depth. The critical shear stress was 0.3 Pa for the top 5 cm and between 1.0 and 2.0 Pa for the lower portion of the core.

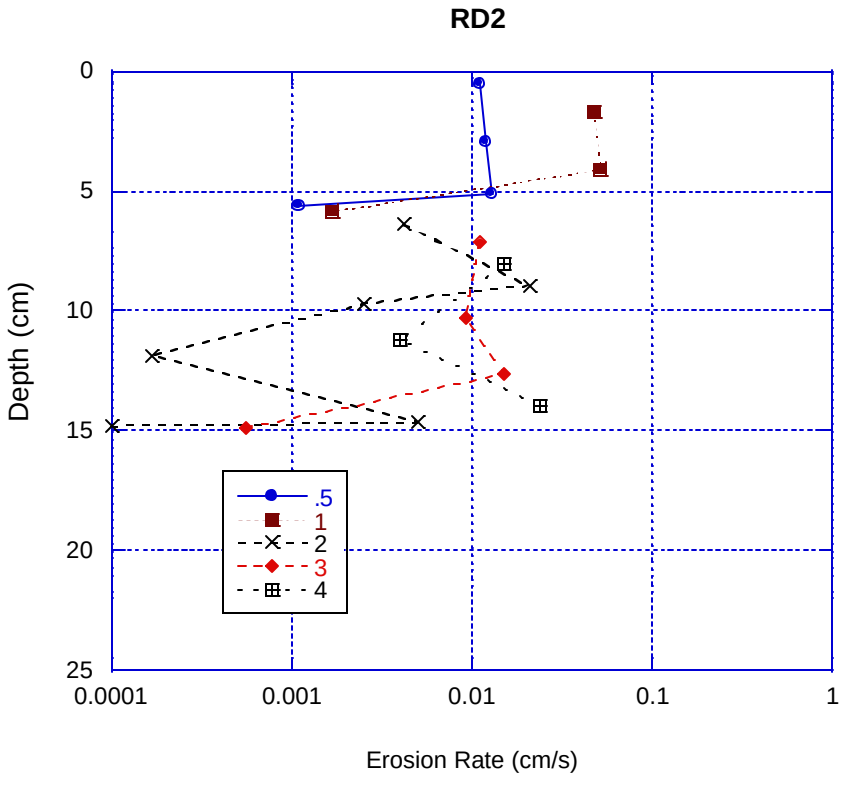

Figure 3.1g

The sample taken from the flood plain next to the channel, RD3, was 17 cm long and was predominantly medium grained sand throughout. The average particle size is shown in Figure 3.1h and the erosion data is shown in Figure 3.1i. The erosion rates are generally constant with depth for both shear stresses run. The critical shear stress was 0.3 to 0.4 Pa throughout the core.

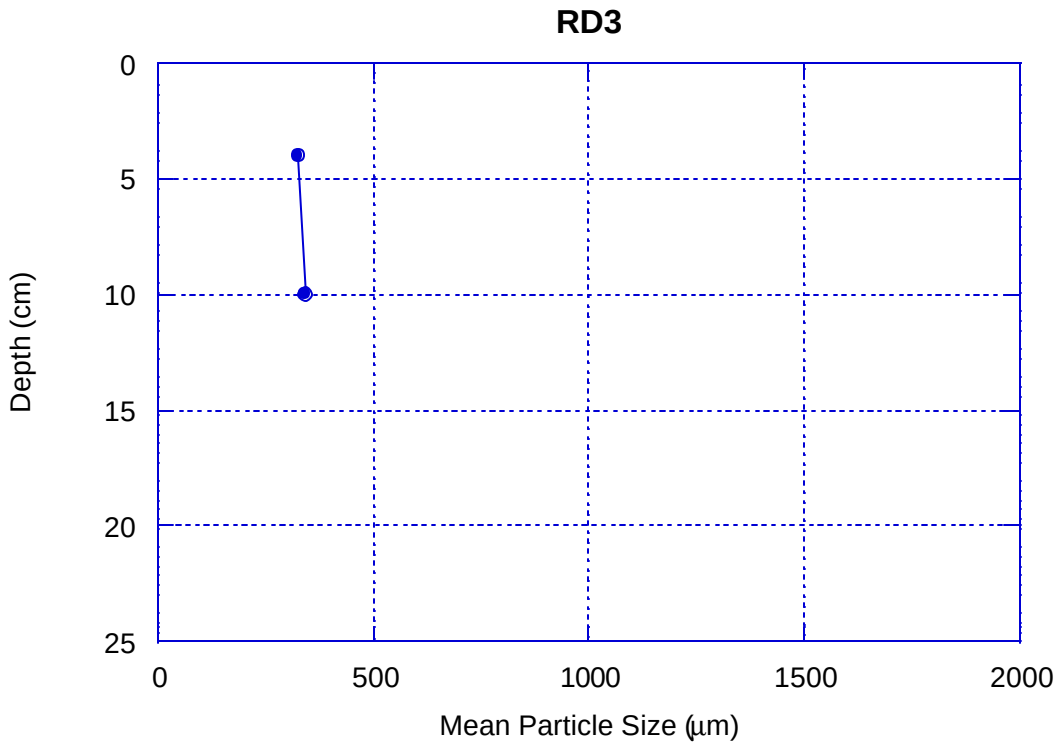

Figure 3.1h

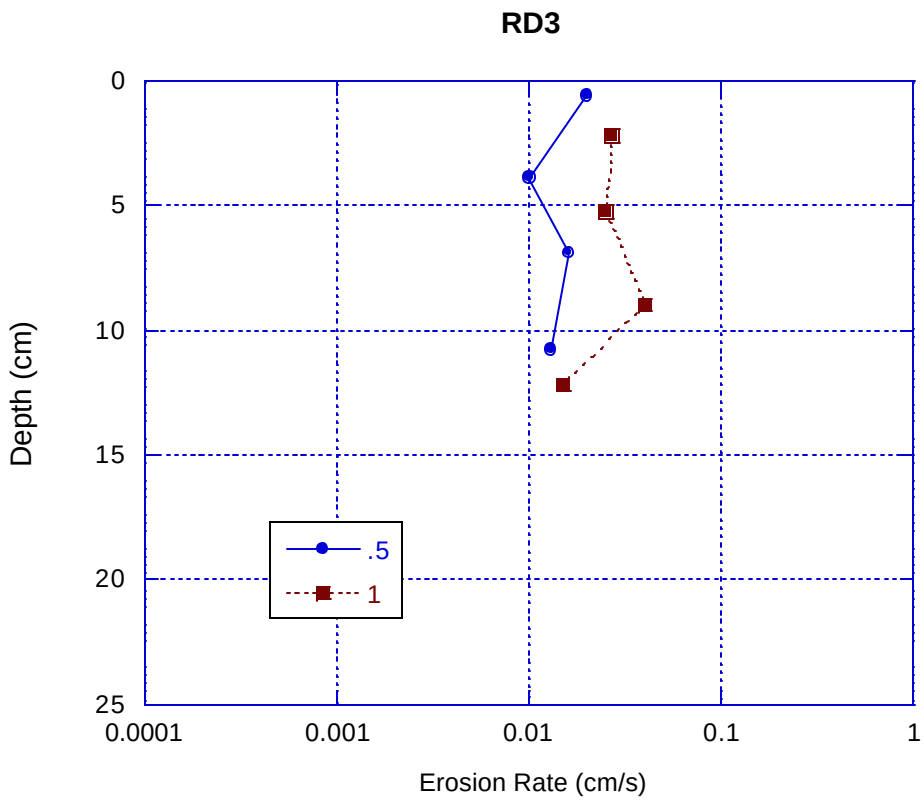

Figure 3.1i

The sample obtained from the upper section of the flood plain, RD4, was 15 cm long. There were three distinct layers observed in this core. The top 0-3 cm was loose organic-rich and dark gray material, the next 3-9 cm was brown silty material, and the remainder of the core was lighter brown in color and clay-like in texture. The average particle size for this sample is shown in Figure 3.1j. The large particle sizes were mainly due to the organic debris mixed in with the sediment.

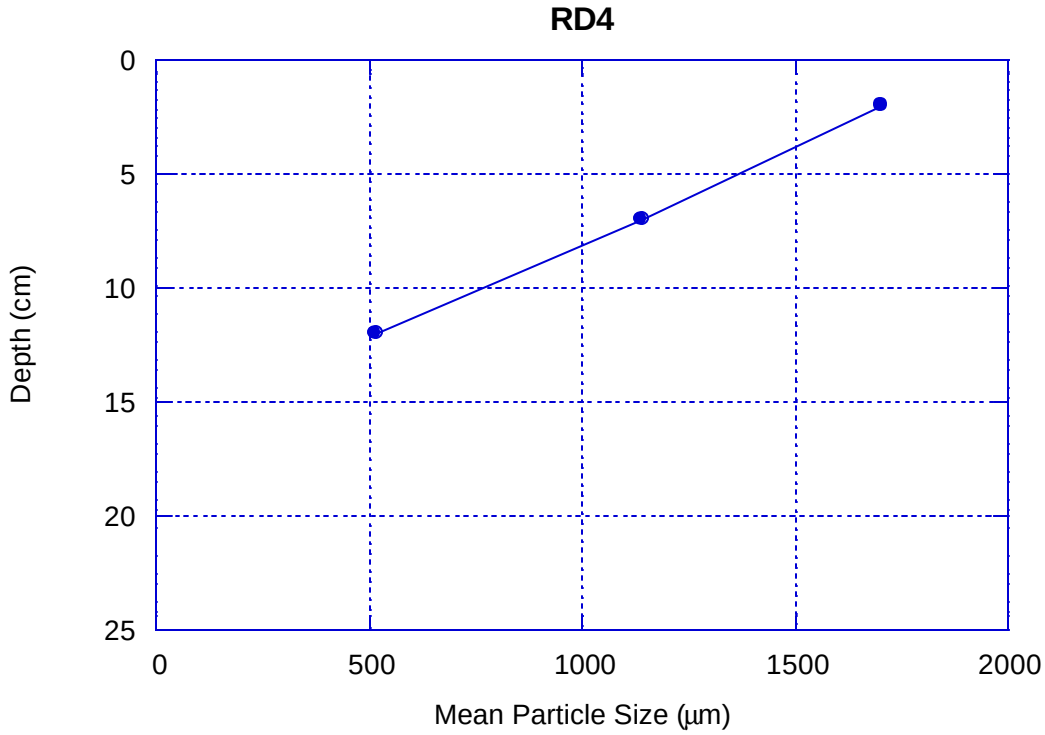

Figure 3.1j

The erosion rates for the RD4 sample decreased by an order of magnitude with depth for the first 7 cm (Figure 3.1k). The remainder of the core had variable erosion rates with depth and the variability was primarily due to the organic debris mixed in with the sediment. The organic debris was mostly comprised of plant material and roots. The very bottom of the core was much more difficult to erode than the upper portion and can be shown by the need to run a 3.0 Pa test in this region. The critical shear stress was 0.2 Pa at 4 to 7 cm deep then increased to 0.5 Pa at 9 to 10 cm.

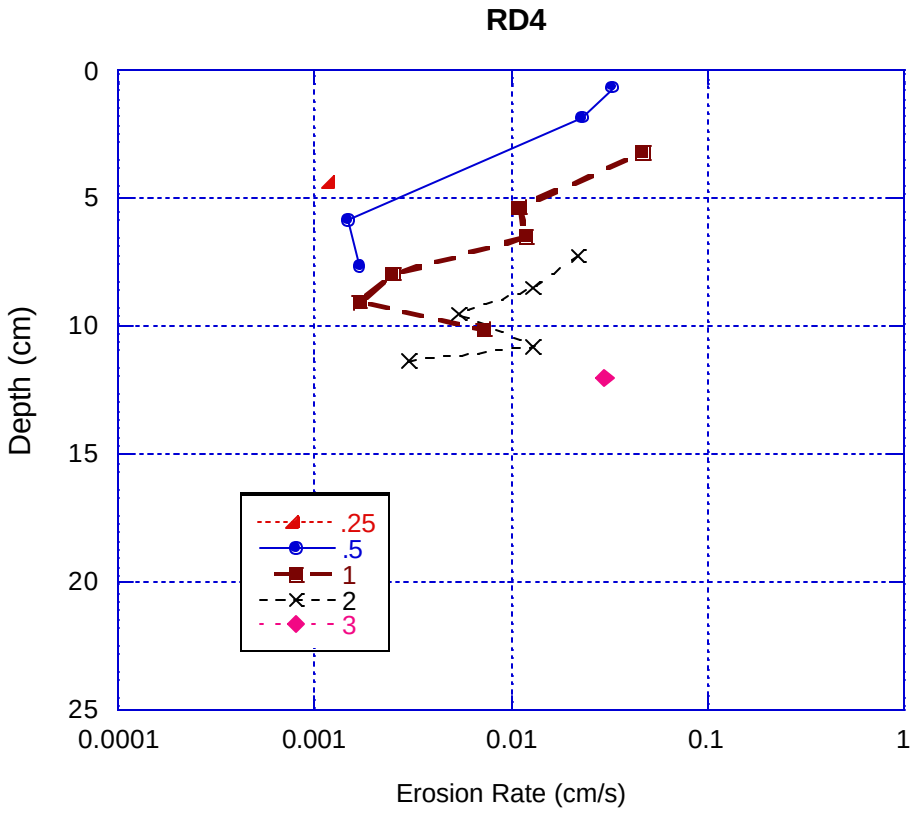

Figure 3.1k

3.1.2 Levee

Only the erosion processes were investigated for this area. Two cores were taken from the levee. One was taken from the bank of the levee and one from the base.

The sample taken from the bank of the Levee, L1, was 16 cm long. The coordinates for this sample are N31^{o}39.628' W106^{o}19.813'. The entire core was mostly sand and small pebbles throughout with some plant debris mixed in. However, the top 2 to 3 cm was mostly sand. The mean particle size for this sample is shown in Figure 3.1l . With the exception of one test at 1.0 Pa near the surface, the core demonstrated very similar erosion properties with depth (Figure

3.1m). The higher erosion rate measured near the surface at 1.0 Pa was due to loose leaf and wood debris mixed in to that layer. The critical shear stress was between 0.2 and 0.3 Pa for all depths.

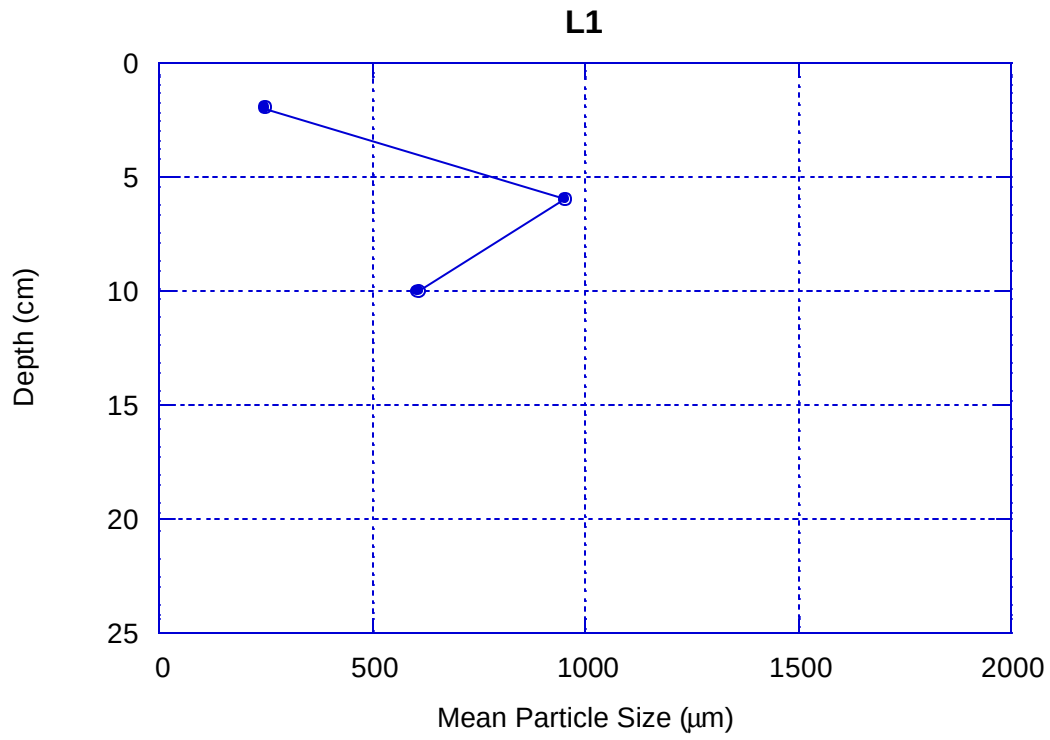

Figure 3.1l

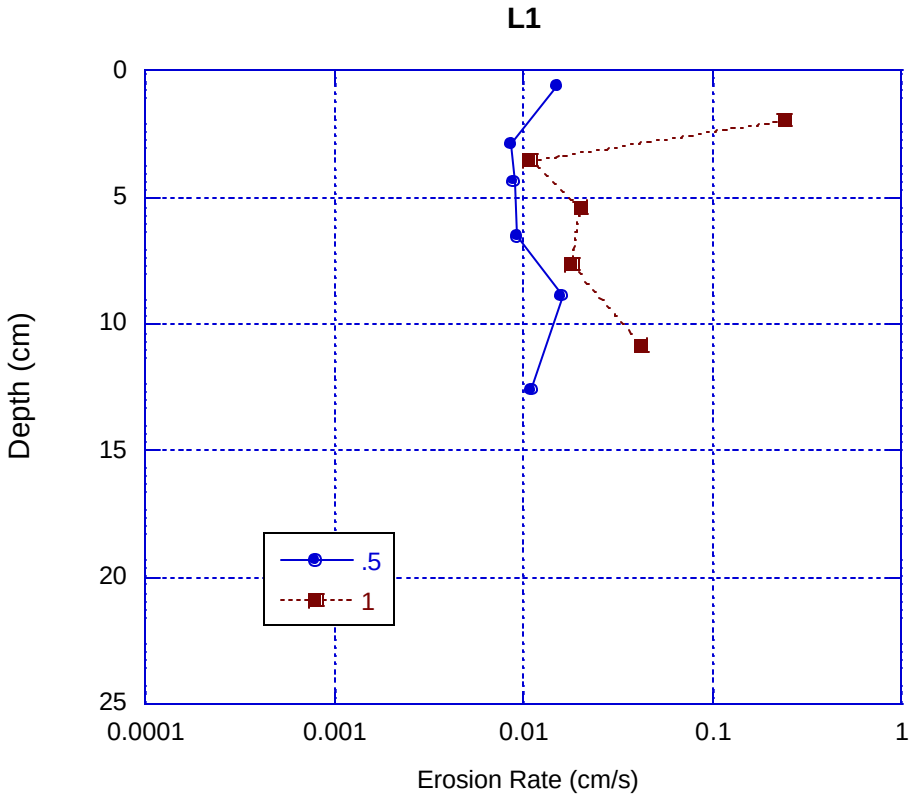

Figure 3.1m

The core sample taken from the base of the Levee, L2, was 19 cm long and was observed to contain uniform, fine sand with some root material near the surface and pebbles mixed throughout. The location of this sample was N31^{o}39.677' W106^{o}19.846'. The average particle size for this sample is shown in Figure 3.1n. The erosion rates were very comparable to that found at site L1 for the same shear stresses applied (Figure 3.1o). The top 2 to 5 cm were somewhat easier to erode than the surface and underlying layers that were found in sample L1. The critical shear stress was also between 0.2 and 0.3 Pa for all depth except 2 to 5 cm where the critical shear stress was between 0.3 and 0.5 Pa.

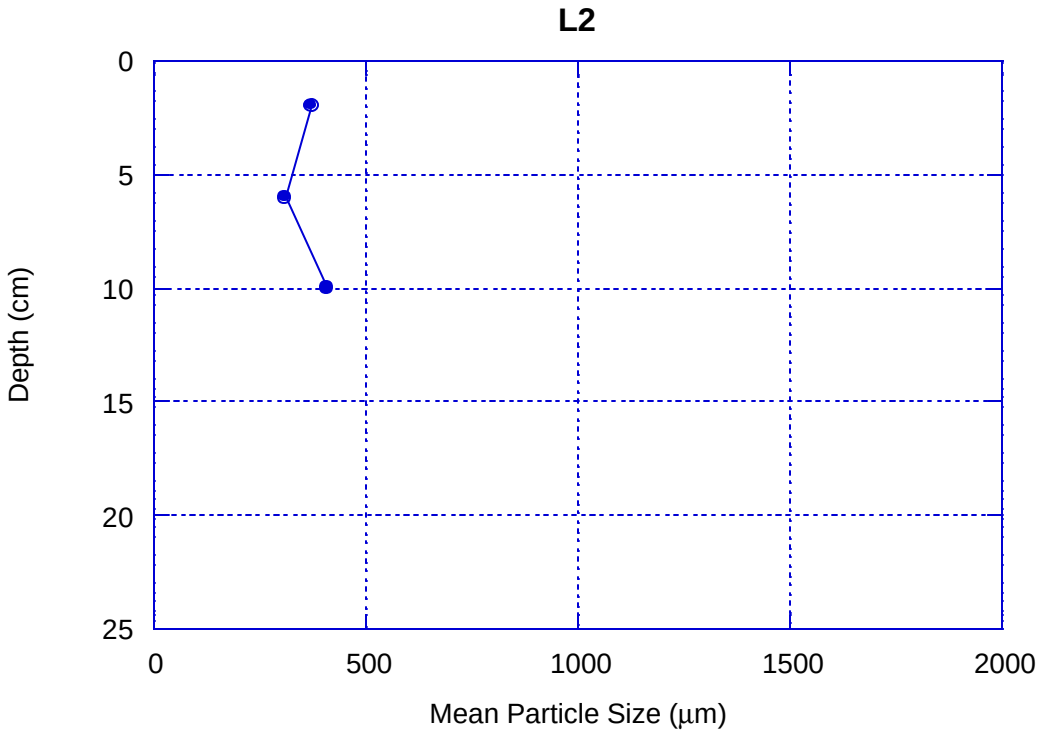
L2
0
5
10
15
20
25
Depth (cm)
0
500
1000
1500
2000
Mean Particle Size (µm)

Figure 3.1n

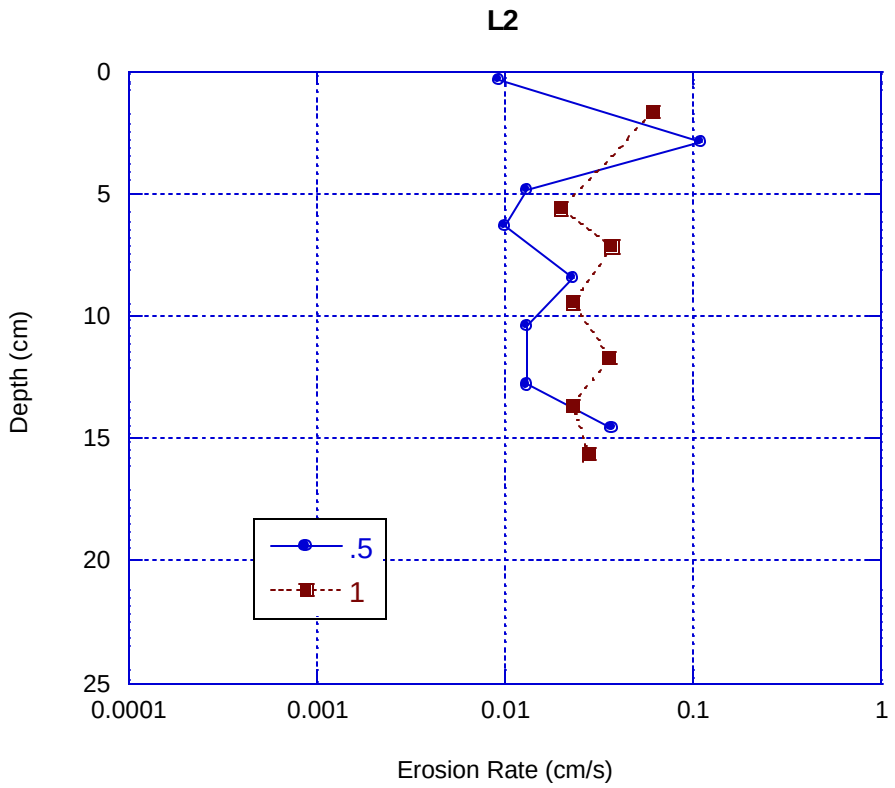

Figure 3.1o

Both Levee samples were similar in composition and erosion properties. The primary difference in composition was the presence of more pebbles in L1 than that observed in L2. Although this created differences in the average particle size, it appears that this difference did not affect erosion properties. In addition, these samples were generally easier to erode at the same shear stresses than the sediments found in the channel and flood plain. The exceptions were the entire sample obtained from the RD3 site and the top 5 cm of the other samples where the erosion rates were very close to the Levee samples.

3.2 Arroyos

Two Arroyos were investigated along the Rio Grande south of El Paso. The mobile flume was used for Alamo Arroyo to get information on in situ cores. Sediments from Balluco Arroyo were taken back to the laboratory in Carlsbad for erosion analysis.

3.2.1 Alamo Arroyo

3.2.1a Morphology

Southeast of El Paso the Rio Grande incises deeper into its floodplain. The stream is incised 2 to 4 meters below the flood plain. Alamo Arroyo enters the Rio Grande from the northeast in a 3-m-deep 20-m-wide channel with a flat floor exhibiting sand bars and scours indicative of recent high-velocity flows (Figure 3.2a). The steep walls of the arroyo and river channel are terraced with the lowest terrace 40 cm above the water level in the Rio Grande and 20 to 40 cm above the arroyo floor. A second terrace is evident in Figure 3.2a approximately 1.2 m above the arroyo floor. The floodplain lies 4 m above the level of water in the Rio Grande and 3 m above the floor of the arroyo. The mouth of the arroyo is an erosional cliff with gravelly arroyo sediment evident in the stream channel. Similar sediments are evident on the south side of the river and it is obvious that the arroyo once crossed the present course of the river. This suggests that the Rio Grande was farther south in the recent past before either channel straightening or avulsion established it in its present course.

There is an obvious change in channel morphology at the arroyo mouth (Figure 3.2a). Downstream (South) of the arroyo, the Rio Grande channel is wider and the channel floor is more irregular, with several bars evident in the channel. The incised channel in which the stream

flows is also wider and terraces are evident along both the American and Mexican sides of the channel.

Above the river channel and terraces, the floodplain is a largely artificial construct that has been leveled and filled in the recent past as is evidenced by the heterogeneous gravels exposed in the stream cuts. Particularly to the north of Alamo Arroyo, the topography and flat terrace is artificial. The terrace is covered with a thicket of tamarisks in which eolian sands have accumulated.

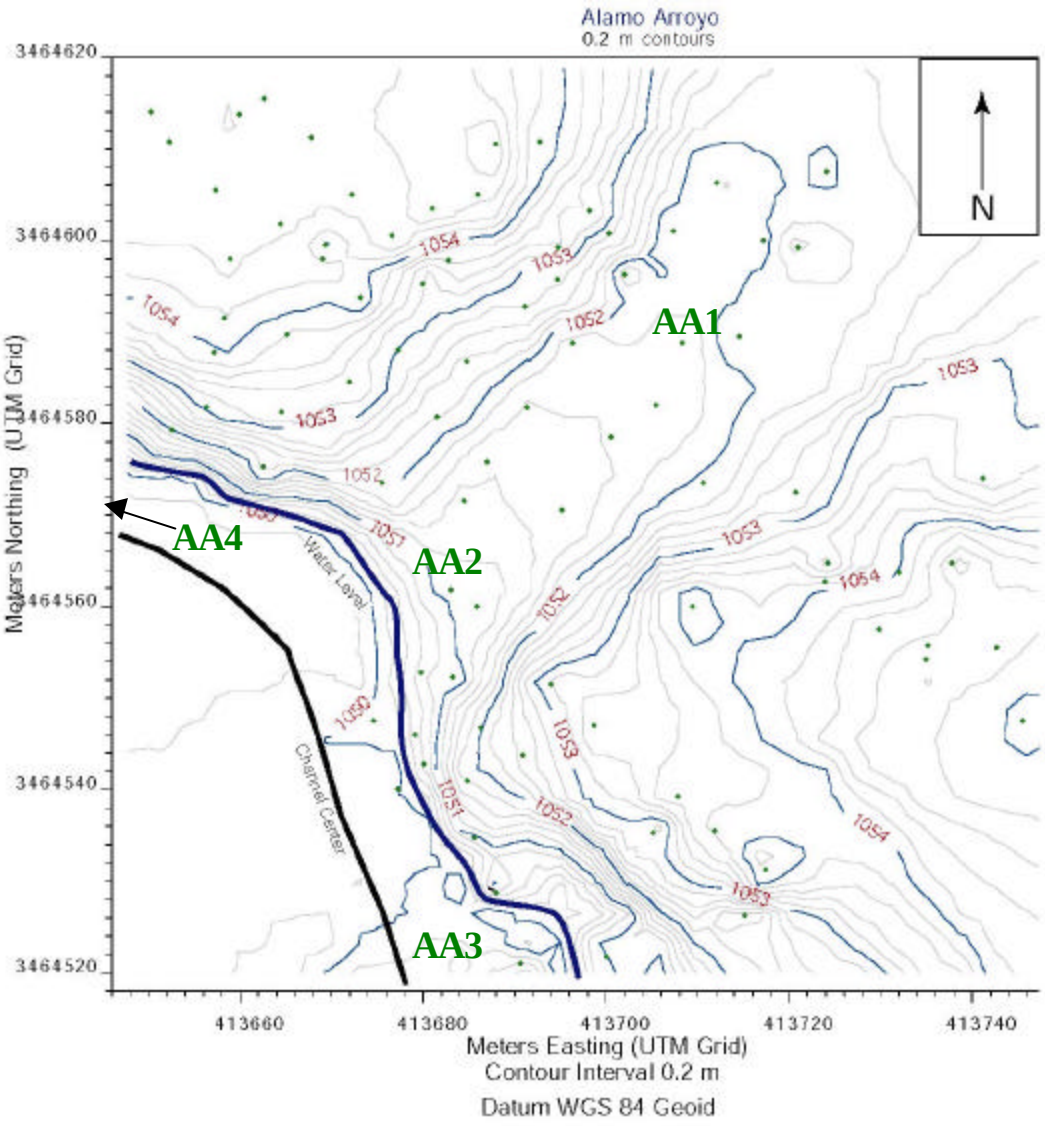

Figure 3.2a. Topographic map of the Arroyo Alamo site with sample locations. Sample location AA4 was northwest of the map coverage area shown.

3.2.1b Electromagnetic Conductivity

EM conductivity was measured in a small area in the arroyo floor to document its electrical properties. The EM conductivity presents a simple pattern of increasing conductivity toward the Rio Grande (Figure 3.2b). This suggests two important features. First, the sediment beneath the arroyo floor is largely heterogeneous. Second, the water content of the sediments increases toward the Rio Grande, and that farther from, and higher above the stream, sediments contain a thick zone with low water content.

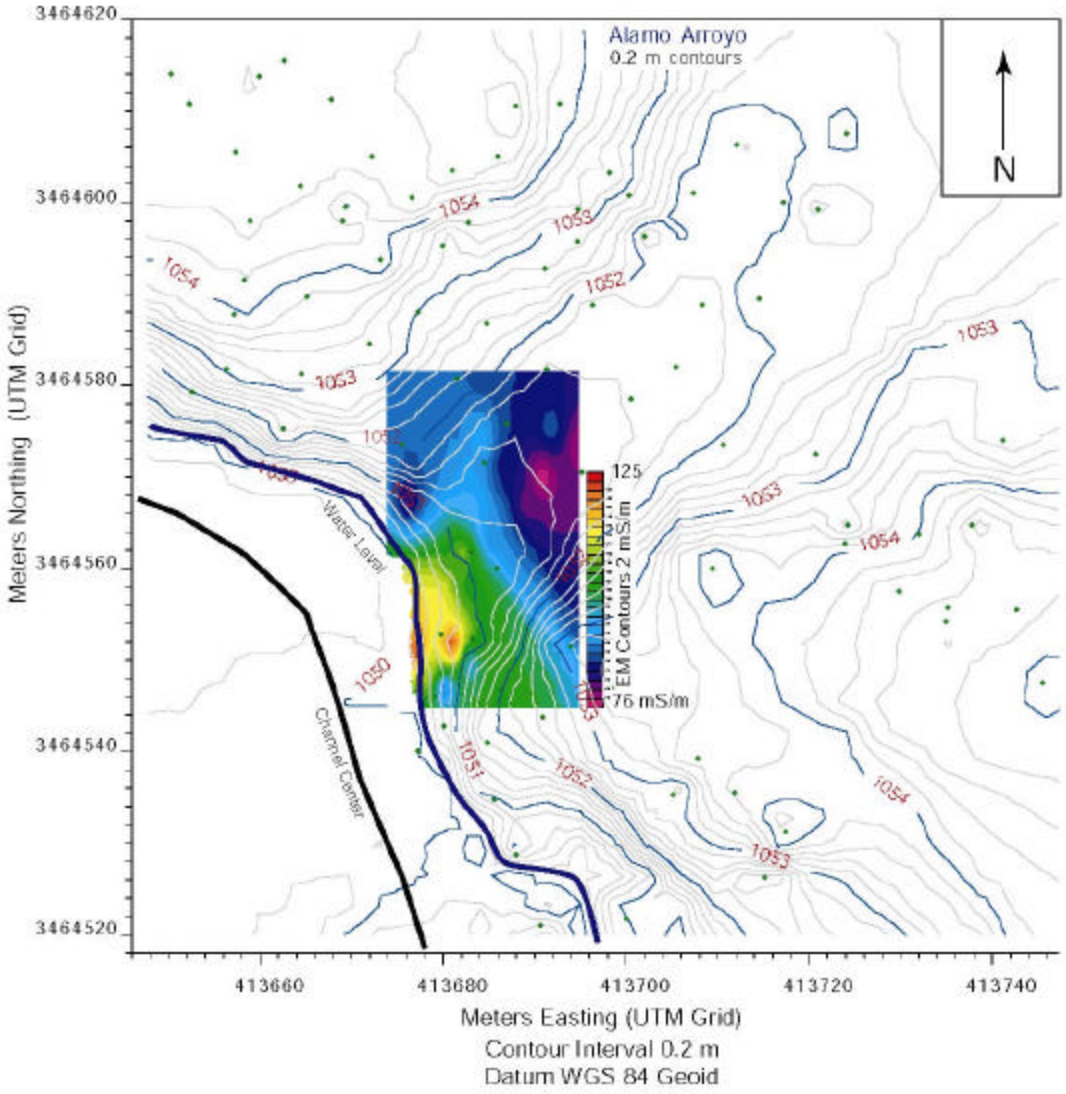

Figure 3.2b. Topographic map with EM conductivities for the Alamo Arroyo site.

3.2.1c Erosion Processes

Four cores were retrieved from the Alamo Arroyo vicinity. Two were from the arroyo channel, AA1 and AA2, one was from the Rio Grande Channel downstream of the arroyo input, AA3, and the fourth site was in the Rio Grande Channel upstream of the arroyo, AA4. The location of these sites is shown in Figure3.2a.

The sample for site AA1 was obtained mid-channel in Alamo Arroyo approximately 100 m from the Rio Grande. The core was 17 cm long and was primarily coarse-grained sand with some larger gravel mixed in. The average particle size is shown in Figure 3.2c. The erosion rates for AA1 were almost constant with depth (Figure 3.2d). The critical shear stress was between 0.15 and 0.2 Pa for the sample.

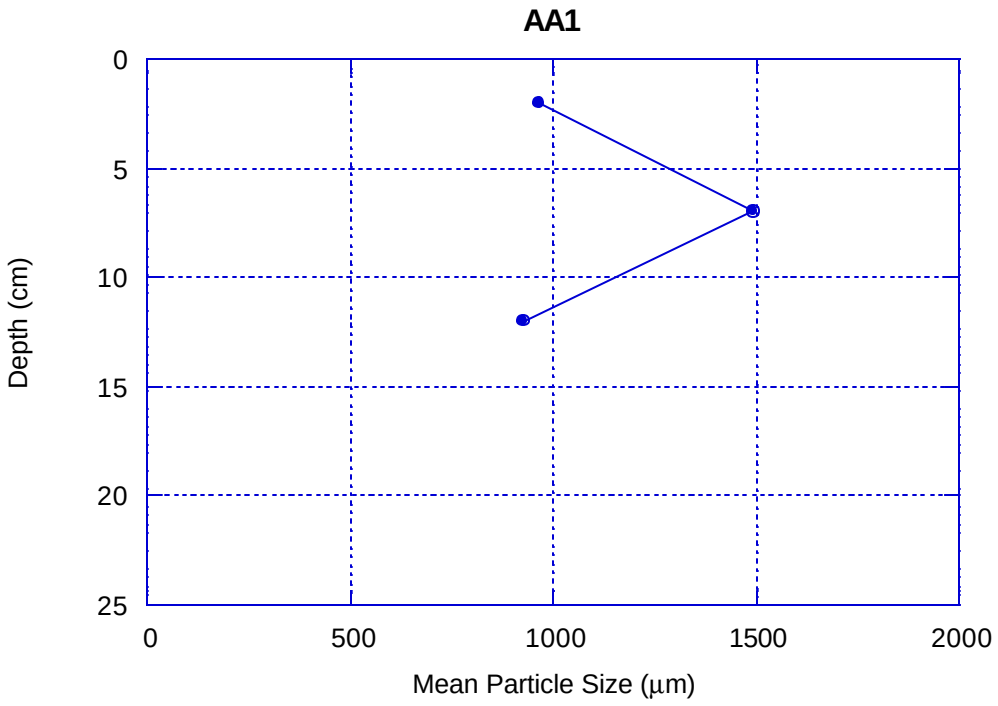

Figure 3.2c

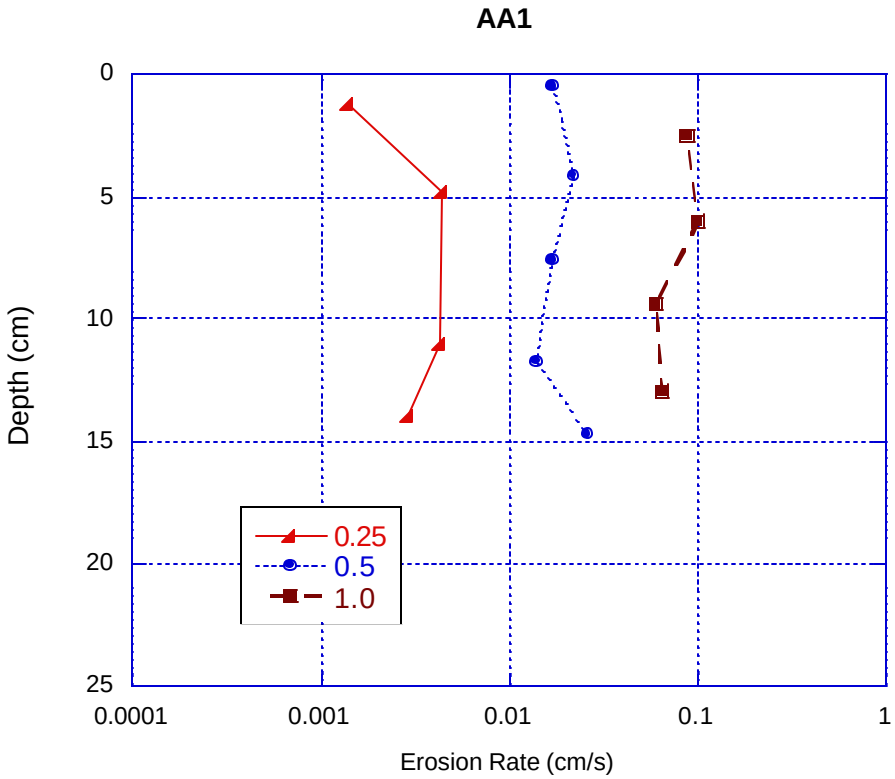

Figure 3.2d

The core from site AA2 was 15 cm long and was visually similar to AA1 in composition. AA2 was taken in the middle of the Alamo Arroyo channel about 2 m from the bank of the Rio Grande. Figure 3.2e shows the mean particle size with depth and Figure 3.2f shows the erosion rates with depth as a function of shear stress. The particle size shows the same trend with depth as AA1. The erosion rates were similar to AA1 for the 0.5 Pa shear stress but the 1.0 Pa shear stress gave erosion rates about 50 to 60% of that found for AA1. The critical shear stress was about 0.3 Pa for the top 10 cm and about 0.2 Pa for the bottom portion of the core.

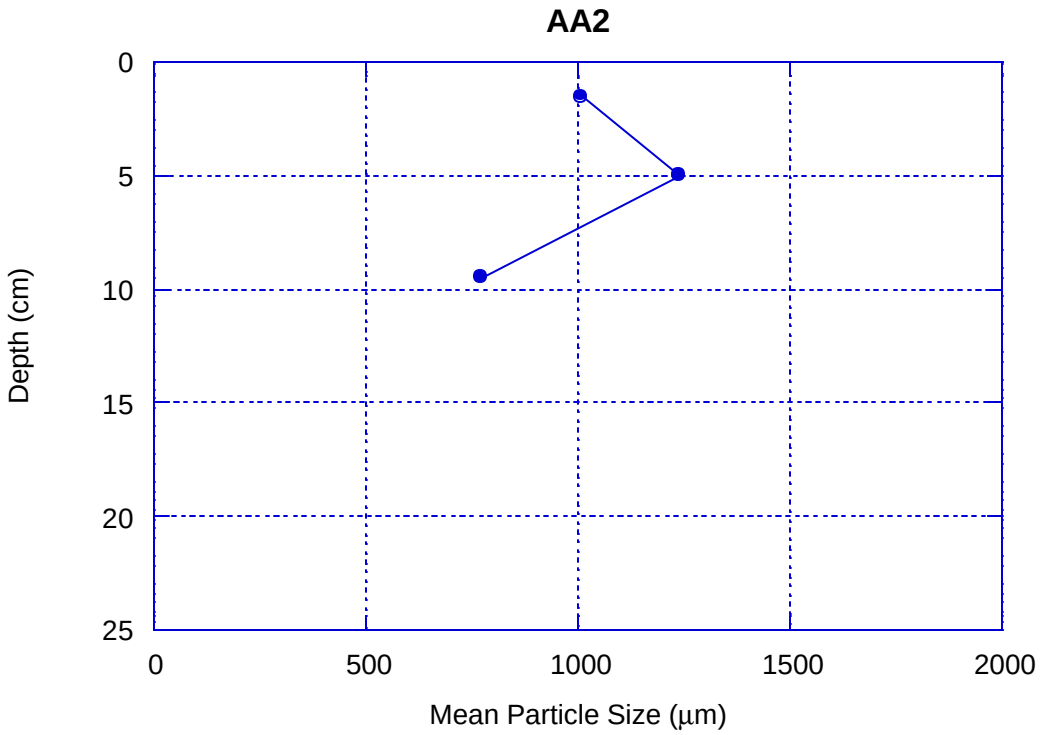
AA2
0
5
10
15
20
25
Depth (cm)
0
500
1000
1500
2000
Mean Particle Size (µm)

Figure 3.2e

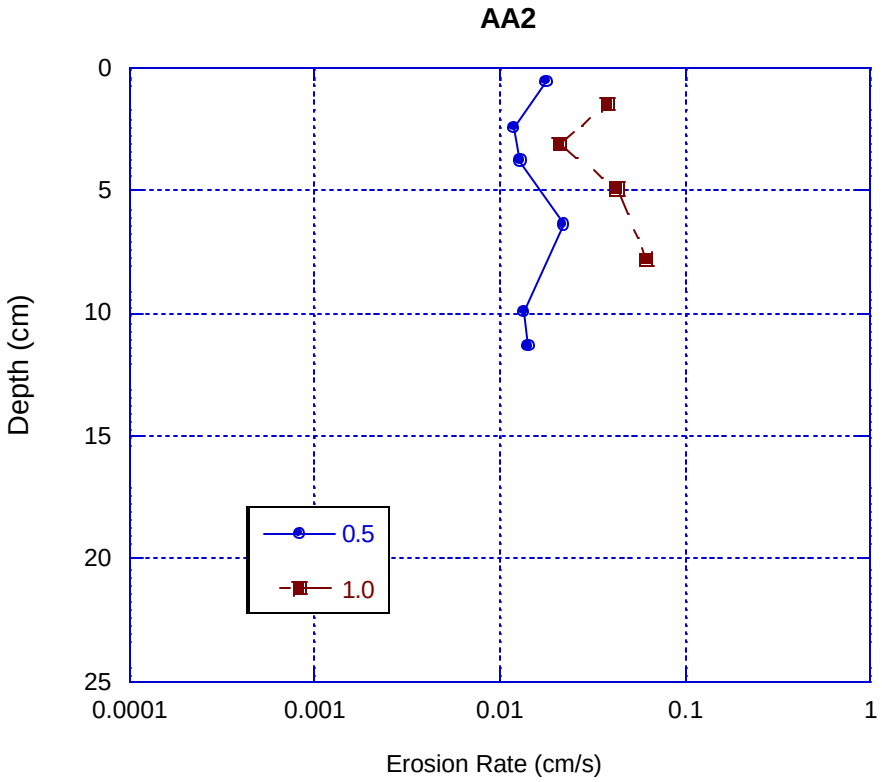

Figure 3.2f

The core from site AA3 was obtained in the Rio Grande mid-channel about 20 m downstream of the Alamo Arroyo confluence. The sample was 21 cm long and generally consisted of medium-grained sand with some coarse material mixed in. The average particle size shown in Figure 3.2g demonstrates that the sediment was uniform with depth. The erosion rates are also generally constant with depth for each shear stress (Figure 3.2h). Even though the grain size is quite different than both AA1 and AA2, the erosion properties are very similar. The critical shear stress was about 0.2 Pa for all depths except for a hard layer at about 3 cm deep that had a critical shear stress of about 0.3 Pa. This layer also showed a decrease in the erosion rate at 0.5 Pa.

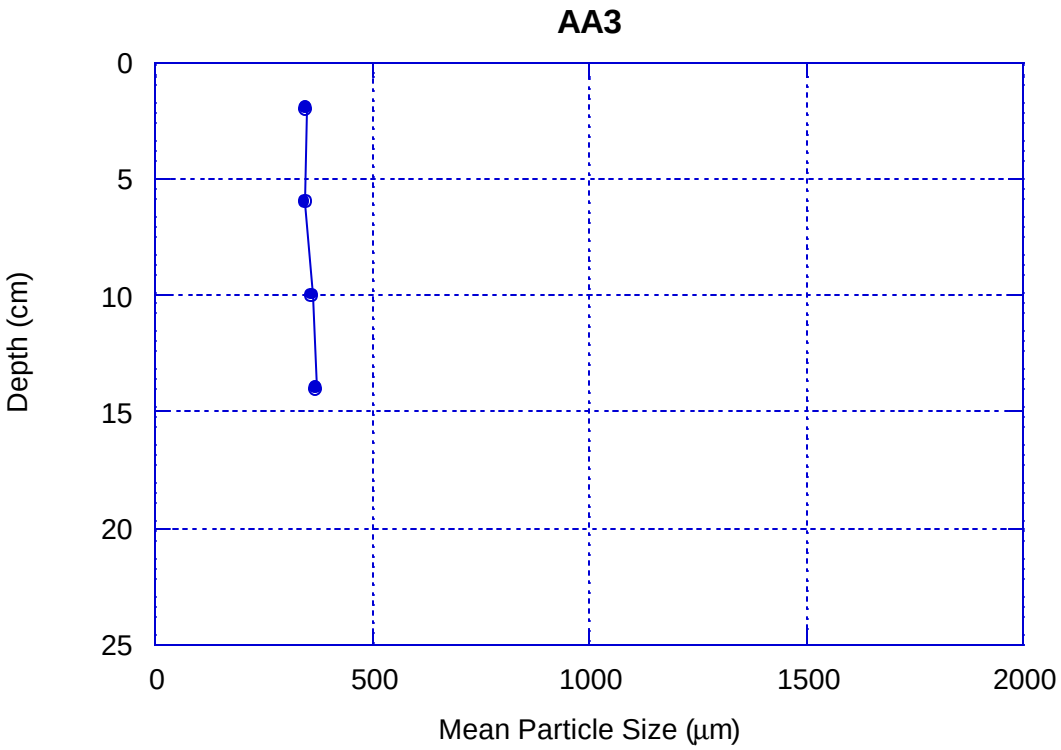
AA3
Depth (cm)
0
5
10
15
20
25
0
500
1000
1500
2000
Mean Particle Size (µm)

Figure 3.2g

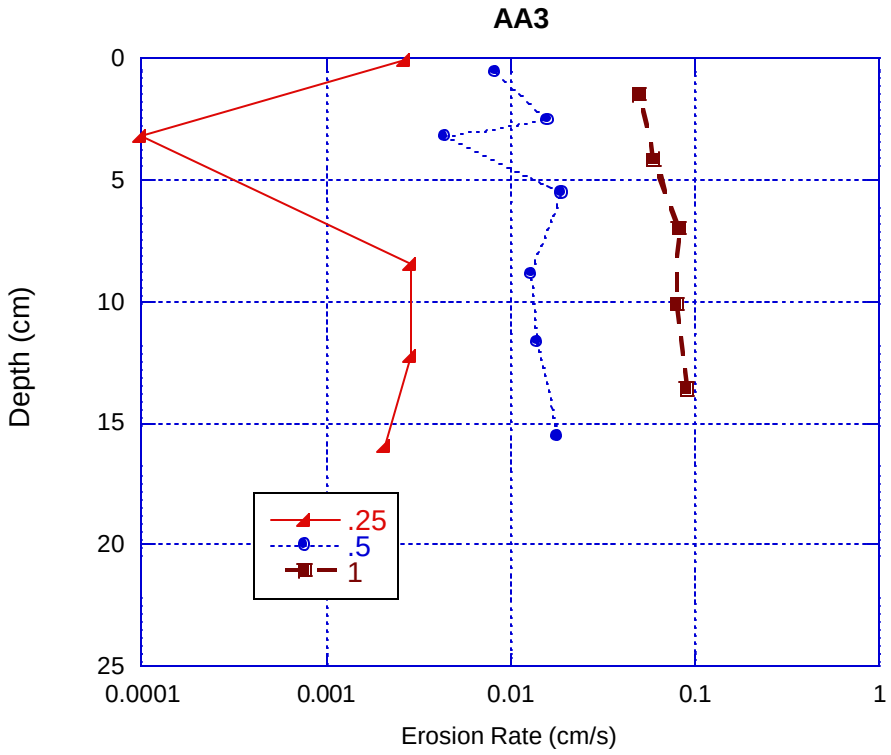

Figure 3.2h

The core sample for site AA4 was taken from the middle of the Rio Grande channel approximately 50 m upstream of the Alamo Arroyo confluence. The core was 25 cm long and from visual observation it was found to contain medium-grained sand with organic rich material mixed in from 11 to 18 cm deep. The particle size was between 285 and 340 µm with the coarser grained material being near the top portion of the core (Figure3.2i). From the distribution (Appendix C), it can be seen that very little coarse material was associated with the upstream site, AA4. The erosion tests also show that the sediment in this region was about a factor of two easier to erode at the same shear stress (Figure 3.2j). In addition, the critical shear stress was less than 0.2 Pa for all depths.

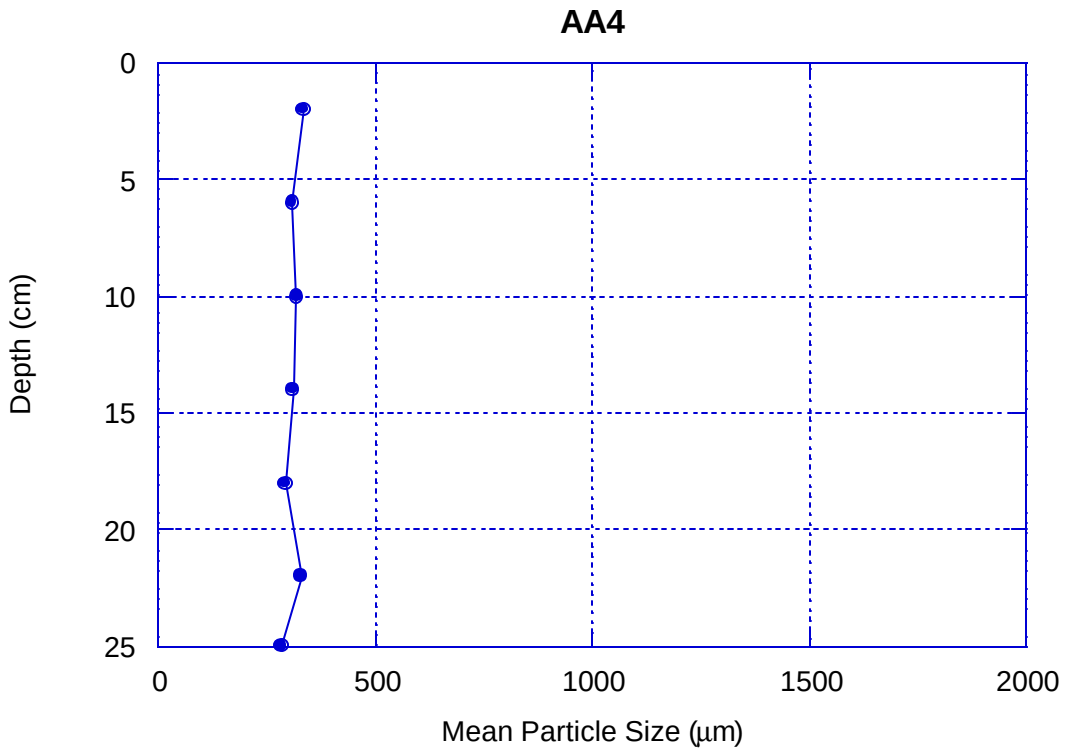
AA4
Depth (cm)
0
5
10
15
20
25
0
500
1000
1500
2000
Mean Particle Size (μm)

Figure 3.2i

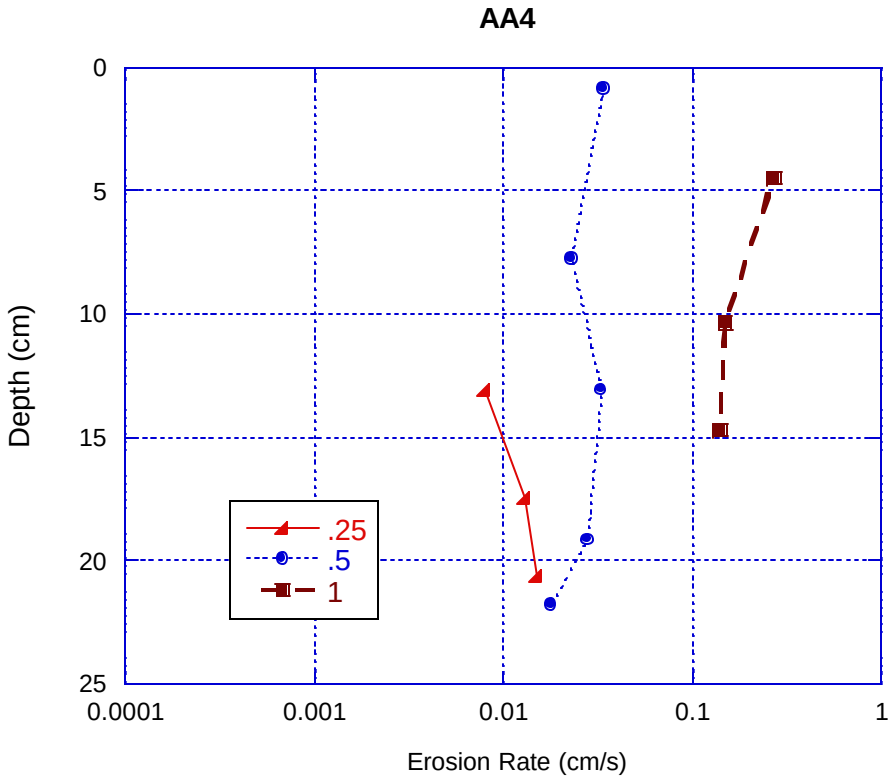

Figure 3.2j

In general, the sediments in the arroyo (AA1 and AA2) were more coarse and difficult to erode than what was found in the Rio Grande channel upstream (AA4). The results also show that the arroyo has introduced material into the Rio Grande by increasing the coarse fraction of the particle size downstream of the confluence (AA3) and causing the sediment in this region to be difficult to erode. The implication is that when large flows in Alamo Arroyo occur, the sediments carried in the flow may deposit in the Rio Grande channel immediately downstream and can remain for an extended period. Since the arroyo sediments are coarser-grained they are more difficult to erode (Roberts et al, 1998) and can cause the flow in the Rio Grande channel to be impeded.

3.2.2 Balluco Arroyo

3.2.2a Morphology

Balluco Arroyo is similar in topography to Alamo Arroyo. The channel is incised 2 m into the surrounding floodplain and is also 20 m wide (Figure 3.2k). The floodplain has been artificially leveled and is a low relief grassy plain. A prominent terrace parallels the floor of the floodplain 60 cm above the floor of the arroyo. The terrace continues along the Rio Grande for 30 m southeast of the arroyo mouth. The arroyo flooded twice during our experiment and the arroyo floor was reshaped. It exhibits upper flow regime features and scours that are often covered by a thin clay drape. Flood water wetted the channel margin 1 m above the arroyo floor. The Rio Grande artificial channel is approximately 10 m wide upstream of the arroyo and is confined in steep unterraced banks.

Downstream of the arroyo mouth the Rio Grande Channel changes shape more than at Alamo Arroyo. The overall channel approaches 25 m wide and contains numerous gravelly bars with intervening narrower channels. During the course of this study the July 17th or 18th flood of Balluco Arroyo established a bar across the Rio Grande that dammed the Rio Grande and increased its depth upstream of the arroyo mouth to over 2 m. Downstream of the arroyo mouth, the stream is 50 to 60 cm deep and flows rapidly across a gravelly bed. The bar also created a backwater that extended up Balluco Arroyo for 80 m. The surface of the bar exposed coarse gravel, coarser that was evident in the arroyo. The bar itself is evident on Figure 3.2k between the water line and 1035.3 meter elevation line. The bar is 32 m wide and extends 100 m downstream from the arroyo mouth. Sediments deposited by the bar are at least 1 m thick and may be 1.5 m thick.

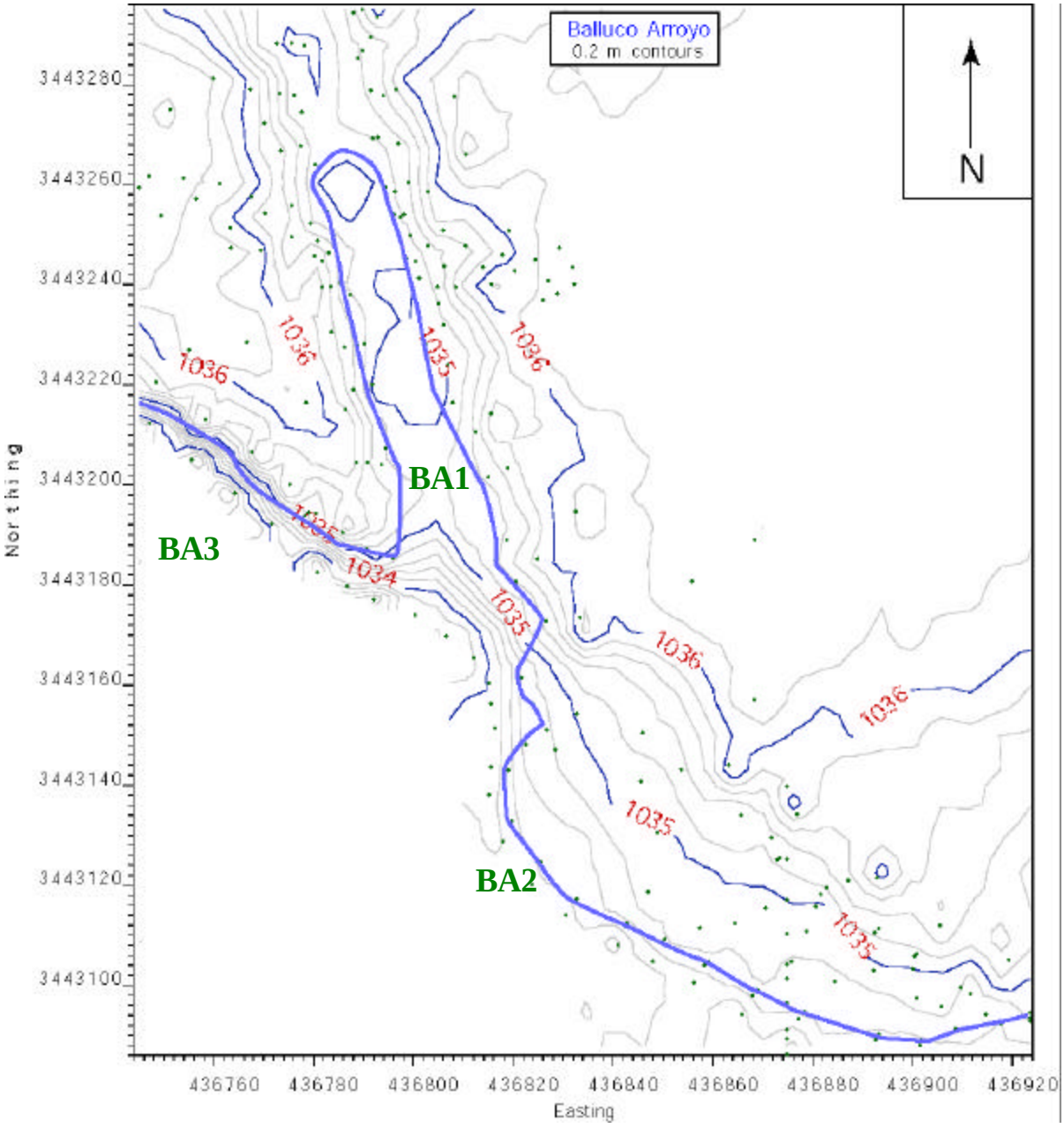

Figure 3.2k. Topographic map of the Balluco Arroyo Site with sample locations.

3.2.2b Erosion Processes

Sediments were taken from three sites at Balluco Arroyo for laboratory studies (Figure 3.2k). The results shown in Table 3.2 show that the erosion potential for site BA1 and BA3 are similar at low shear stresses with site BA2 being much more difficult to erode. Also, it was noted that the material in sample BA2 eroded such that the finer sand would be scoured around the larger gravel and the gravel would not erode until the finer material significantly exposed the gravel to the flow.

Table 3.2. Laboratory Results

	Upstream of Balluco Arroyo (BA3)	Balluco Arroyo (BA1)	Downstream of Balluco Arroyo (BA2)
Critical Shear	0.3 Pa	0.3 Pa	0.65 Pa
Shear Stress	----------*Erosion Rates*----------		
0.5 Pa	0.0016 cm/s	0.0019 cm/s	-
1.0 Pa	0.012 cm/s	0.032 cm/s	0.0017 cm/s
2.0 Pa	-	-	0.038 cm/s
Mean Particle Size (μm)	122	787	2195

Comparing these results to the case at Alamo Arroyo, one might expect BA3 to be the easiest to erode. However, from the particle size data, BA3 contains some silt and clay material mixed in with 200-300 μm sand. This causes the sample to be more cohesive in comparison to the upstream site in Alamo Arroyo (AA4). Also, the sample from BA1 is not nearly as coarse as BA2. Sample BA2 contains a significant amount of gravel material that increases its overall

resistance to erosion. The size distribution for these samples (Figure 3.2l) shows that they are both bi-modal and contain material with a peak near 300 µm and a peak between 1000 and 5000 µm. The difference is that the BA1 sample contains more of the finer material and the BA2 sample contains more of the coarse, gravel material. Therefore, when the Arroyo flooded, the bulk material introduced into the Rio Grande Channel separated by size class. The finer material contained in the 300 µm peak was washed downstream while the much coarser material remained since it is much more difficult to erode. This is very similar to what was noted during the laboratory erosion tests.

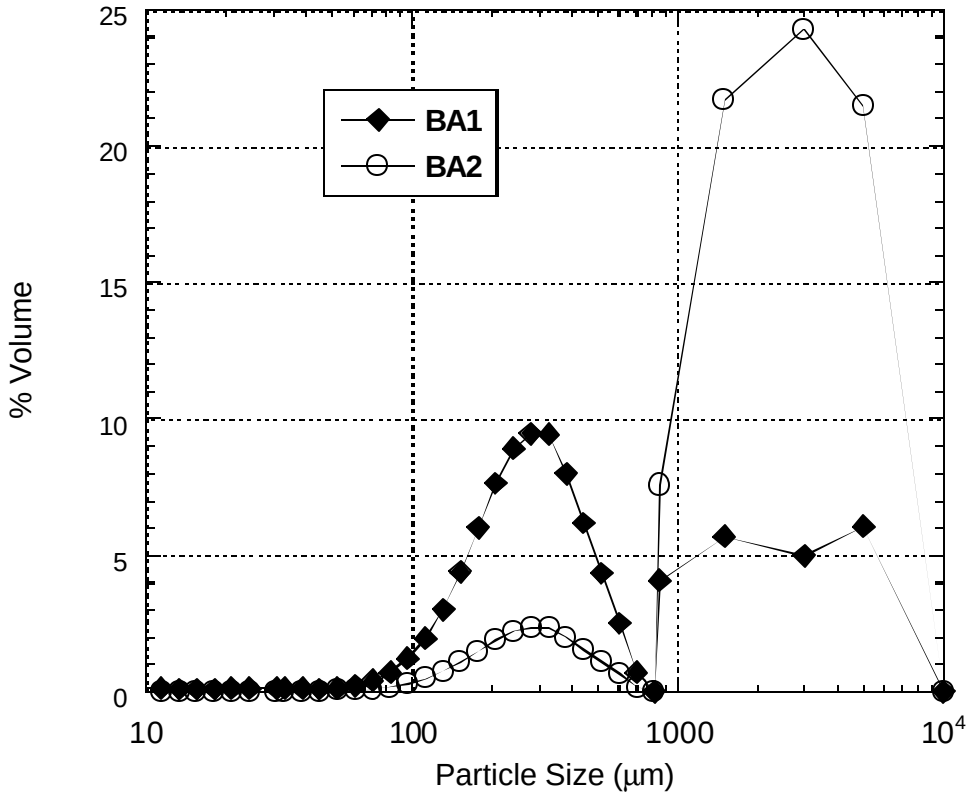

Figure 3.2l

4. Conclusions

The study demonstrates the utility of this unique technology in both engineered sites and natural channels. The flume results correlated well with results from both EM-conductivity and can be related to changes in topographic features as well as channel morphology. This technology is of particular importance to the Rio Grande along the border because so much of the sediment load is easily eroded fine-grained sand. This means that additions of silt and clay or gravel can reduce the erodibility of the stream and change its behavior.

There are two key results from the Riverside Dam site. First, interstratified sand and clay drastically reduced the erodibility of the sediment along the banks and in the floodplain. Because the EM device has proven its utility in mapping these features, locations that will be more resistant to erosion can be quickly identified and their erosion potential characterized. Second, the levees at this site erode under similar shear stresses to the channel sands surrounding them.

At both Alamo and Balluco Arroyos, the presence of coarse material makes the channel-filling sediments more difficult to erode downstream from the arroyos. The critical shear stresses required to erode channel sediments were at least two-times greater downstream from the arroyos. This highlights a natural process that probably affects the Rio Grande along much of its length. Accretion of more poorly erodable bars within the channel occurs during low-flow years. These changes were associated with widening of the channel and the formation of mid-channel and side-channel bars.

Altogether, the demonstration focused on two specific sediment issues related to water management, public health, and economic development. These issues were re-mobilization of

sediments and possible contaminants at Riverside Dam and arroyo sediment load effects on the engineered Rio Grande channel in the El Paso Valley. The Riverside Dam area was chosen for the demonstration because it was a characteristic site, readily accessible, and was not a major area of contamination. The arroyo sites were chosen because they represent many of the arroyo characteristics on both sides of the border. Future studies regarding highly contaminated areas would require additional training and planning for sediment handling and operations. In addition, the areas of high contamination require political support from the stakeholders on both sides of the border because of issues related to responsibility for the remediation of those sites. A technology transfer to a border agency would allow for better planning with regard to technical and political issues and significantly aid in the determination of the sediment properties related to water contamination, management, and use along the border.

5. References

Jepsen, R., Roberts, J., Lucero, A., and Chapin M. 2001. Canaveral ODMDS Dredged Material Erosion Rate Analysis. SAND 2001-1989. Sandia National Laboratories, Albuquerque, NM

McNiel, J.D., 1992. Rapid accurate mapping of soil salinity by electromagnetic ground conductivity meters. In *Advancmetns in methods of measuring soil physical properties: bringing theory into practice.* (ed G.C. Topp, and Reynolds, W. D.) Special Publication No. 30, pp. 209-229. Soil Science Society of America, Madison Wisconsin.

Roberts, J., Jepsen, R., Gotthard, D. and Lick, W. 1998. "Effects of particle size and bulk density on erosion of quartz particles." Journal of Hydraulic Engineering, ASCE, 124(12), 1261-1267.

Roberts, J. and Jepsen, R. 2001a. Development for the Optional Use of Circular Core Tubes with the High Shear Stress Flume. SAND2001-0424. Sandia National Labs, Albuquerque, NM.

Roberts, J., Jepsen, R., Bryan, C., Chapin, M.. 2001b. Boston Harbor Sediment Study. SAND 2001-2226. Sandia National Laboratories, Albuquerque, NM

Schlichting, H., 1979. *Boundary-Layer Theory*. Seventh ed, McGraw-Hill.

Appendix A

Raw GPS Data

Riverside Flood Basin GPS Data

Data collected using Trimble 3100 GPS System
Datum is WGS 84
Coordinates are UTM Grid east and north

Point Name	North (m)	East (m)	Elevation (m)
RIVLV	3503539.632	373902.738	1095.21
RIVL0001	3503534.715	373903.788	1095.35
RIVL0002	3503526.318	373902.878	1095.31
RIVL0003	3503521.939	373902.344	1095.3
RIVL0004	3503516.499	373901.547	1095.28
RIVL0005	3503510.583	373900.542	1095.22
RIVL0006	3503502.122	373899.336	1095.18
RIVL0007	3503493.711	373898.087	1095.21
RIVL0008	3503487.599	373896.96	1095.12
RIVL0009	3503480.449	373895.96	1095.11
RIVL0010	3503469.643	373893.653	1094.93
RIVL0011	3503460.322	373893.79	1094.89
RIVL0012	3503453.594	373897.755	1095.08
RIEM0001	3503508.692	373900.794	1095.23
RIEM0002	3503500.261	373899.526	1095.23
RIEM0003	3503492.588	373898.438	1095.22
RIEM0004	3503485.907	373897.485	1095.19
RIEM0005	3503479.226	373896.64	1095.13
RIEM0006	3503468.939	373895.489	1095
RIEM0007	3503460.699	373896.41	1095.13
RIEM0008	3503453.601	373897.928	1095.09
RILV0013	3503441.359	373902.975	1095.05
RILV0014	3503435.357	373894.249	1093.59
RILV0015	3503440.443	373890.85	1093.68
RILV0016	3503446.526	373890.837	1093.68
RILV0017	3503451.528	373891.629	1093.67
RILV0018	3503455.947	373891.318	1093.69
RILV0019	3503463.896	373890.641	1093.72
RILV0020	3503474.542	373890.071	1093.76
RILV0021	3503482.384	373891.812	1093.87
RILV0022	3503490.798	373893.271	1094.02
RILV0023	3503500.556	373895.739	1094.21
RIRD0001	3503500.109	373891.793	1094.04
RIRD0002	3503498.314	373888.456	1093.87
RIRD0003	3503491.031	373888.908	1093.9
RIRD0004	3503488.261	373884.988	1093.78
RIRD0005	3503482.06	373886.632	1093.65
RIRD0006	3503475.605	373883.009	1093.61
RIRD0007	3503470.67	373884.305	1093.64
RIRD0008	3503466.911	373881.371	1093.56
RIRD0009	3503460.073	373882.634	1093.51
RIRD0010	3503455.543	373878.343	1093.53
RIBAR001	3503462.926	373876.434	1093.53
RIBA0001	3503467.038	373872.212	1093.58
RIBA0002	3503472.773	373870.421	1093.61
RIBA0003	3503478.042	373871.143	1093.65
RIBA0004	3503481.292	373869.521	1093.62
RIBA0005	3503484.16	373866.772	1093.57
RIBA0006	3503487.231	373868.587	1093.62
RIBA0007	3503491.771	373870.027	1093.6
RIBA0008	3503496.444	373872.441	1093.76
RIBA0009	3503502.836	373875.514	1093.83
RIBA0010	3503508.345	373878.747	1094.11

Riverside Flood Basin GPS Data

Data collected using Trimble 3100 GPS System
Datum is WGS 84
Coordinates are UTM Grid east and north

Point Name	North (m)	East (m)	Elevation (m)
RIBA0011	3503511.048	373882.523	1094.16
RIBA0012	3503517.23	373884.864	1094.16
RIBA0013	3503523.594	373890.523	1094.23
RIBA0014	3503527.538	373894.555	1094.52
RIBA0015	3503530.388	373899.601	1094.8
RIEM0009	3503451.546	373889.399	1093.68
RIEM0010	3503458.276	373889.034	1093.54
RIEM0011	3503467.053	373889.295	1093.68
RIEM0012	3503475.662	373889.422	1093.81
RIEM0013	3503484.378	373890.021	1093.76
RIEM0014	3503491.247	373890.871	1094.01
RIEM0015	3503500.606	373888.98	1093.83
RIEM0016	3503484.94	373885.698	1093.77
RIEM0017	3503476.505	373884.253	1093.67
RIEM0018	3503467.983	373883.108	1093.63
RIEM0019	3503457.36	373882.045	1093.54
RIEM0020	3503451.321	373881.844	1093.51
RIEM0021	3503450.787	373876.285	1093.53
RIEM0022	3503457.22	373875.755	1093.48
RIEM0023	3503468.454	373876.981	1093.57
RIEM0024	3503477.252	373877.888	1093.65
RIEM0025	3503486.475	373879.772	1093.66
RIEM0026	3503494.99	373882.129	1093.72
RIEM0027	3503502.175	373883.861	1093.83
RIT20001	3503544.502	373896.472	1093.54
RIT20002	3503542.24	373891.859	1093.48
RIT20003	3503540.306	373890.052	1093.63
RIT20004	3503534.4	373888.051	1093.62
RIT20005	3503527.86	373886.074	1093.59
RIT20006	3503525.683	373889.893	1093.93
RIT20007	3503528.555	373891.512	1093.98
RIT20008	3503532.785	373893.116	1093.93
RIT20009	3503536.044	373896.122	1093.83
RIT20010	3503539.294	373898.827	1094.02
RIT20011	3503522.681	373887.155	1093.91
RIT20012	3503522.486	373884.163	1093.69
RIT20013	3503518.465	373883.767	1093.83
RIT20014	3503516.503	373880.641	1093.51
RIT20015	3503509.158	373877.865	1093.74
RIT20016	3503512.092	373874.538	1093.34
RIT20018	3503503.324	373874.319	1093.54
RIT20019	3503503.511	373866.972	1093.38
RIT20020	3503498.554	373861.883	1093.38
RIT20021	3503495.558	373859.2	1093.46
RIT20022	3503491.923	373856.293	1093.51
RIT20023	3503489.066	373852.584	1093.49
RIT20024	3503494.442	373847.95	1093.18
RIT20025	3503498.508	373846.433	1093.08
RIT20026	3503502.474	373843.745	1093.04
RIT20027	3503506.518	373839.25	1093.14
RIT20028	3503506.684	373837.008	1093.19
RIT20029	3503499.035	373835.127	1093.28
RIT20030	3503493.905	373837.394	1093.63
RIT20031	3503488.943	373841.146	1093.71
RIT20032	3503482.386	373846.122	1093.63

Riverside Flood Basin GPS Data

Data collected using Trimble 3100 GPS System
Datum is WGS 84
Coordinates are UTM Grid east and north

Point Name	North (m)	East (m)	Elevation (m)
RIT20033	3503478.089	373850.102	1093.5
RIT20034	3503466.69	373857.14	1093.56
RIT20035	3503460.09	373863.379	1093.76
RIT20036	3503449.998	373871.353	1093.56
RIT20037	3503442.492	373877.788	1093.63
RIT20038	3503506.868	373877.395	1093.99
RIEM0028	3503506.79	373877.399	1093.99
RIEM0029	3503498.104	373871.782	1093.64
RIEM0030	3503489.079	373866.165	1093.53
RIEM0031	3503479.368	373864.473	1093.48
RIEM0032	3503469.916	373863.99	1093.46
RIEM0033	3503457.714	373867.232	1093.49
RIEM0034	3503449.725	373871.21	1093.54
RIEM0035	3503447.031	373864.579	1092.71
RIEM0036	3503443.229	373857.176	1092.89
RIEM0037	3503440.733	373847.375	1093.02
RIEM0038	3503445.736	373843.544	1092.98
RIEM0039	3503447.773	373850.329	1092.95
RIEM0040	3503451.838	373859.494	1092.71
RIEM0041	3503456.851	373858.64	1092.61
RIEM0042	3503456.452	373852.151	1093.06
RIEM0043	3503455.85	373844.789	1093.15
RIEM0044	3503462.588	373844.159	1092.96
RIEM0045	3503466.903	373837.065	1093.01
RIEM0046	3503464.95	373849.273	1092.74
RIEM0047	3503465.665	373853.896	1092.58
RIEM0048	3503471.883	373848.938	1092.73
RIEM0049	3503471.919	373844.148	1092.8
RIEM0050	3503473.446	373835.287	1092.99
RIEM0051	3503476.897	373842.038	1092.8
RIEM0052	3503481.917	373841.774	1092.72
RIEM0053	3503480.766	373837.531	1092.77
RIEM0054	3503483.996	373828.899	1093.01
RIEM0055	3503490.888	373825.77	1093.01
RIRIV001	3503492.759	373823.14	1092.52
RIRI0001	3503489.003	373822.413	1092.52
RIRI0002	3503482.937	373826.267	1092.59
RIRI0003	3503479.718	373828.544	1092.54
RIRI0004	3503473.778	373831.178	1092.44
RIRI0005	3503465.771	373833.233	1092.5
RISA0001	3503463.769	373832.794	1092.46
RISA0002	3503463.146	373834.867	1092.84
RIEM0056	3503492.579	373834.017	1092.9
RIEM0057	3503496.388	373837.812	1093.51
RIEM0058	3503499.3	373846.577	1093.06
RIEM0059	3503503.914	373853.258	1092.66
RIEM0060	3503508.751	373849.302	1092.67
RIEM0061	3503500.412	373839.005	1093.26
RISA0003	3503467.441	373857.672	1093.52
RIRI0008	3503517.685	373876.594	1092.54
RIRI0009	3503512.116	373872.748	1092.62
RIRI0010	3503505.257	373866.642	1092.56
RIRI0011	3503510.165	373849.139	1092.56
7784	3503527.451	373888.721	1093.84

Arroyo Alamo GPS Data

Data collected using Trimble 3100 GPS System
Datum is WGS 84
Coordinates are UTM Grid east and north

Point Name	North (m)	East (m)	Elevation (m)
ACHAN001	3464606.13	413712.11	1051.77
ACHA0001	3464601.1	413707.376	1051.7
ACHA0002	3464596.16	413702.028	1051.63
ACHA0003	3464588.73	413696.378	1051.52
ACHA0004	3464581.66	413691.305	1051.49
ACHA0005	3464575.82	413687.026	1051.34
ACHA0006	3464571.55	413684.496	1051.29
ACHA0007	3464561.7	413683.022	1051.13
ACHA0008	3464552.68	413679.812	1050.85
ACHA0009	3464547.53	413674.625	1050.82
ACHA0010	3464542.83	413680.094	1050.74
ACHA0011	3464545.94	413679.166	1050.77
ACHA0012	3464552.19	413683.216	1050.87
ACHA0013	3464559.92	413685.833	1051.04
ACHA0014	3464570.42	413695.185	1051.48
ACHA0015	3464578.42	413700.544	1051.61
ACHA0016	3464588.72	413708.334	1051.63
ACHA0017	3464599.99	413717.176	1051.81
ACHA0018	3464607.61	413724.088	1051.96
ROAD0019	3464552.01	413748.258	1054.99
ROAD0020	3464547.62	413745.576	1055.1
ROAD0021	3464555.61	413742.715	1054.72
ROAD0022	3464555.68	413735.153	1054.42
ROAD0023	3464563.8	413732.073	1053.84
ROAD0024	3464564.87	413724.251	1053.14
ROAD0025	3464572.61	413720.791	1052.57
ROAD0026	3464573.5	413710.637	1051.98
ROAD0027	3464582.11	413705.454	1051.65
ROAD0028	3464586.7	413684.796	1052.36
ROAD0029	3464595.31	413680.009	1052.84
ROAD0030	3464599.45	413669.339	1053.98
ROAD0031	3464613.84	413659.932	1054.36
ROAD0032	3464614.09	413650.298	1054.45
EDG10033	3464610.75	413652.355	1054.48
EDG10034	3464605.6	413657.36	1054.45
EDG10035	3464598.07	413658.931	1054.47
EDG10036	3464591.46	413658.266	1054.28
EDG10037	3464587.84	413657.176	1054.03
EDG10038	3464581.75	413656.36	1053.21
EDG10039	3464579.17	413652.591	1052.21
EDG10040	3464575.25	413662.516	1052.27
EDG10041	3464581.18	413664.557	1053.34
EDG10042	3464589.72	413665.161	1053.77

Arroyo Alamo GPS Data

Data collected using Trimble 3100 GPS System
Datum is WGS 84
Coordinates are UTM Grid east and north

Point Name	North (m)	East (m)	Elevation (m)
EDG10043	3464601.84	413664.464	1054.5
EDG10044	3464597.92	413669.101	1054.42
EDG10045	3464593.73	413673.143	1054.19
EDG10046	3464587.93	413677.327	1052.94
EDG10047	3464584.45	413671.966	1053.41
EDG10048	3464580.78	413681.497	1052.24
EDG10049	3464573.49	413675.52	1052.09
EDG10050	3464615.49	413662.651	1054.45
EDG10051	3464611.2	413667.825	1054.53
EDG10052	3464605.02	413672.237	1054.51
EDG10053	3464600.49	413676.637	1054.67
EDG10054	3464603.48	413681.07	1054.8
EDG10055	3464605.08	413686.027	1054.86
EDG10056	3464610.4	413687.99	1055.13
EDG10057	3464610.78	413692.75	1053.91
EDG10058	3464597.72	413682.783	1053.53
T2ED0059	3464592.78	413691.185	1052.86
T2ED0060	3464595.81	413694.734	1052.87
T2ED0061	3464600.72	413700.318	1052.72
T2ED0062	3464603.15	413698.174	1053.44
T2ED0063	3464599.31	413694.752	1053.43
T1ED0064	3464589.38	413714.563	1052.22
T1ED0065	3464599.24	413720.995	1052.53
T1ED0066	3464611.57	413736.476	1052.41
T1ED0067	3464588.9	413756.812	1052.88
T1ED0068	3464580.91	413747.941	1052.92
T1ED0069	3464573.94	413741.218	1053.01
EDG20070	3464564.64	413737.74	1054.93
EDG20071	3464554.32	413734.941	1054.98
EDG20072	3464557.58	413729.807	1054.59
EDG20073	3464562.75	413723.898	1054.19
EDG20074	3464560.02	413709.477	1054.22
EDG20075	3464551.62	413693.976	1053.43
EDG20076	3464547.01	413698.687	1053.7
EDG20077	3464539.29	413707.849	1053.84
EDG20078	3464535.59	413711.87	1054.02
EDG20079	3464531.35	413717.49	1054.53
RTED0080	3464543.82	413690.93	1052.51
RTED0081	3464535.31	413705.136	1052.64
RTED0082	3464526.34	413715.161	1051.89
RTED0083	3464521.66	413700.088	1051.82
RTED0084	3464520.96	413690.692	1051.8
RTED0085	3464528.69	413688.053	1052.13
RTED0086	3464534.7	413685.582	1052.33
RTED0087	3464540.99	413684.897	1052.38

Arroyo Alamo GPS Data

Data collected using Trimble 3100 GPS System
Datum is WGS 84
Coordinates are UTM Grid east and north

Point Name	North (m)	East (m)	Elevation (m)
RTED0088	3464546.66	413686.327	1052.35
RTED0089	3464539.89	413677.287	1050.24
	3464571.5	413650.25	1049.75
	3464571.25	413651.375	1049.75
	3464571	413652.188	1049.75
	3464570.5	413653.188	1049.75
	3464570	413654.531	1049.75
	3464569.25	413655.719	1049.75
	3464568.75	413657	1049.75
	3464567.75	413658.406	1049.75
	3464567	413659.906	1049.75
	3464566	413661.375	1049.75
	3464565	413663.375	1049.75
	3464564	413664.531	1049.75
	3464563	413666	1049.75
	3464562.25	413667.188	1049.75
	3464561	413668.406	1049.75
	3464560	413670.156	1049.75
	3464558	413671.688	1049.75
	3464555.75	413673.406	1049.75
	3464553.75	413674.625	1049.75
	3464551.75	413675.625	1049.75
	3464549	413676.594	1049.75
	3464547.25	413677.406	1049.75
	3464545	413677.844	1049.75
	3464542.75	413678.563	1049.75
	3464540	413679.406	1049.75
	3464538.25	413680.313	1049.75
	3464536.5	413681.375	1049.75
	3464534.5	413683.438	1049.75
	3464532.75	413685.219	1049.75
	3464530.5	413687.125	1049.75
	3464529	413688.719	1049.75
	3464527.25	413690.094	1049.75
	3464525.75	413691.25	1049.75
	3464524.5	413692.469	1049.75
	3464523.5	413694	1049.75
	3464522.5	413694.844	1049.75
	3464521.25	413696.156	1049.75
	3464520.5	413696.344	1049.75
	3464520	413696.375	1049.75

Arroyo Balluco GPS Data

Data collected using Trimble 3100 GPS System
Datum is WGS 84
Coordinates are UTM Grid east and north

Point Name	North (m)	East (m)	Elevation (m)
BASE	3443238.18	436828.862	1036.619
ROAD0001	3443240.07	436832.214	1036.76
ROAD0002	3443243.57	436831.915	1036.763
ROAD0003	3443240.8	436826.989	1036.617
ROAD0004	3443244.99	436824.47	1036.438
ROAD0005	3443242.65	436820.33	1036.108
ROAD0006	3443246	436817.78	1035.993
ROAD0007	3443243.49	436813.925	1035.617
ROAD0008	3443247.63	436810.472	1035.622
ROAD0009	3443243.75	436806.201	1035.521
ROAD0010	3443247.78	436802.885	1035.165
ROAD0011	3443244.82	436800.439	1035.318
T1000012	3443241.34	436801.196	1035.397
T1000013	3443241.16	436799.231	1034.757
T1000014	3443245.13	436798.55	1034.917
T1000015	3443249.72	436799.473	1035.32
T1000016	3443254.06	436798.153	1035.333
T1000017	3443253.91	436796.04	1034.751
T1000018	3443253.53	436797.449	1035.346
T1000019	3443253.53	436797.472	1035.316
T2000020	3443239.56	436804.87	1035.287
T2000021	3443236.25	436805.084	1035.104
T2000022	3443231.94	436806.057	1035.108
T2000023	3443224.01	436806.907	1035.124
T2000024	3443216.55	436807.873	1035.392
T2000025	3443210.38	436812.52	1035.136
T2000026	3443201.56	436815.083	1035.075
T2000027	3443189.02	436818.734	1035.169
T2000028	3443185.09	436816.502	1035.464
T2000029	3443180.86	436820.563	1035.044
T2000030	3443172.83	436826.593	1035.52
RIV00031	3443161.39	436821.579	1034.713
RIV00032	3443156.13	436824.04	1034.766
RIV00033	3443150.99	436826.732	1034.751
RIV00034	3443147	436828.399	1034.756
RIV00035	3443147.89	436822.539	1034.717
RIV00036	3443143.01	436819.03	1034.637
RIV00037	3443132.87	436819.617	1034.631
RIV00038	3443124.39	436825.548	1034.54
RIV00039	3443117.29	436832.773	1034.563
RIV00040	3443111.68	436842.421	1034.485
RIV00041	3443112.14	436842.704	1034.819

Arroyo Balluco GPS Data

Data collected using Trimble 3100 GPS System
Datum is WGS 84
Coordinates are UTM Grid east and north

Point Name	North (m)	East (m)	Elevation (m)
RIV00042	3443108.68	436849.951	1034.59
RIV00043	3443109.19	436850.43	1035.043
RIV00044	3443103.94	436858.315	1034.582
RIV00045	3443104.71	436859.231	1035.212
RIV00046	3443098.11	436867.957	1034.673
RIV00047	3443099.08	436869.044	1035.004
RIV00048	3443093.24	436877.116	1034.323
RIV00049	3443094.81	436878.384	1034.938
RIV00050	3443088.92	436892.609	1034.332
RIV00051	3443090.35	436893.27	1034.583
RIV00052	3443087.94	436901.446	1034.273
RIV00053	3443088.99	436901.684	1034.501
RIV00054	3443090.83	436908.61	1034.322
RIV00055	3443091.29	436908.537	1034.602
RIV00056	3443092.15	436917.599	1034.166
RIV00057	3443092.43	436917.545	1034.624
RIV00058	3443092.85	436923.491	1034.098
RIV00059	3443093.6	436923.558	1034.751
RIV00060	3443094.61	436923.529	1034.931
BAR00061	3443094.15	436914.686	1034.626
BAR00062	3443098.13	436911.599	1034.645
BAR00063	3443095.73	436905.722	1034.823
BAR00064	3443097.6	436900.713	1034.854
BAR00065	3443103.19	436900.05	1034.794
BAR00066	3443103.09	436892.21	1034.833
BAR00067	3443100.71	436884.409	1034.632
BAR00068	3443104.73	436875.677	1034.664
BAR00069	3443110.64	436878.839	1034.861
BAR00070	3443115.65	436880.648	1034.827
BAR00071	3443115.41	436870.521	1034.797
BAR00072	3443112.29	436864.388	1034.738
BAR00073	3443111.53	436857.389	1035.014
BAR00074	3443118.68	436847.013	1035.096
BAR00075	3443130.49	436848.9	1034.842
BAR00076	3443140.69	436845.611	1035.031
BAR00077	3443154.16	436832.778	1035.243
BAR00078	3443150.54	436845.9	1035.461
BAR00079	3443143.11	436853.614	1035.296
BAR00080	3443133.91	436865.635	1035.287
BAR00081	3443129.5	436871.704	1035.22
BAR00082	3443125.61	436873.382	1035.515
BAR00083	3443124.92	436872.904	1035.034
BAR00084	3443118.16	436881.621	1034.966
BAR00085	3443119.44	436882.736	1035.669
BAR00086	3443120.99	436887.02	1035.817

Arroyo Balluco GPS Data

Data collected using Trimble 3100 GPS System
Datum is WGS 84
Coordinates are UTM Grid east and north

Point Name	North (m)	East (m)	Elevation (m)
BAR00087	3443111.13	436893.161	1035.683
BAR00088	3443110.47	436892.419	1034.867
BAR00089	3443105.71	436900.307	1034.958
BAR00090	3443106.35	436900.838	1035.682
BAR00091	3443099.61	436909.637	1034.652
T1000092	3443104.99	436919.274	1036.029
T1000093	3443111.92	436905.416	1035.972
T1000094	3443121.5	436892.894	1036.465
T1000095	3443134.29	436876.919	1036.576
T1000096	3443144.07	436863.129	1036.55
T1000097	3443156.93	436868.273	1036.786
T1000098	3443173.55	436874.669	1036.635
T1000099	3443188.9	436868.381	1036.76
T1000100	3443180.7	436855.836	1036.693
T1000101	3443173.39	436833.414	1036.871
T1000102	3443185.36	436824.906	1036.625
T1000103	3443194.76	436832.565	1036.797
T1000104	3443203.31	436818.894	1036.454
T1000105	3443214.32	436815.633	1036.586
T1000106	3443239.61	436808.563	1036.471
T1000107	3443240	436815.732	1036.581
T1000108	3443247.32	436829.224	1036.727
T1000109	3443250.85	436819.124	1036.625
T1000110	3443250.75	436805.968	1036.702
T1000111	3443258.41	436802.87	1036.545
T1000112	3443266.02	436810.541	1037.193
T1000113	3443277.58	436808.223	1037.086
T1000114	3443278.99	436796.564	1036.832
T1000115	3443293.55	436792.837	1036.692
TT200116	3443295.01	436789.732	1035.534
TT200117	3443294.28	436787.959	1035.491
TT200118	3443289.52	436791.431	1035.63
TT200119	3443286.82	436789.879	1035.551
TT200120	3443278.87	436791.424	1035.525
TT200121	3443277.7	436794.058	1035.534
TT200122	3443269.54	436792.949	1035.353
TT200123	3443268.33	436796.962	1035.475
TT200124	3443260.53	436799.038	1035.414
TT200125	3443258.38	436796.379	1035.466
TT200126	3443251.48	436796.637	1034.84
TT200127	3443259.6	436794.402	1034.843
TT200128	3443269.33	436791.893	1034.914
TT200129	3443285.22	436788.866	1034.957
1AM10130	3443288.37	436775.655	1034.969
1AM10131	3443287.78	436778.175	1034.849

Arroyo Balluco GPS Data

Data collected using Trimble 3100 GPS System
Datum is WGS 84
Coordinates are UTM Grid east and north

Point Name	North (m)	East (m)	Elevation (m)
ARO00132	3443288.22	436772.675	1034.817
ARO00133	3443277.71	436776.175	1034.809
ARO00134	3443274.39	436777.713	1034.74
ARO00135	3443263.94	436780.354	1034.687
ARO00136	3443254.67	436782.687	1034.543
ARO00137	3443249.89	436784.011	1034.628
ARO00138	3443237.98	436787.422	1034.409
ARO00139	3443228.37	436790.287	1034.445
ARO00140	3443227.97	436802.433	1034.64
ARO00141	3443219.88	436791.805	1034.465
ARO00142	3443216.84	436805.178	1034.569
ARO00143	3443207.17	436794.48	1034.467
ARO00144	3443185.47	436795.947	1034.748
T1000145	3443186.97	436790.636	1036.04
T1000146	3443190.56	436785.834	1036.306
T1000147	3443194.32	436780.503	1036.184
T1000148	3443194.54	436779.024	1035.454
71000149	3443193.84	436778.269	1034.566
SAM20150	3443193.79	436778.268	1034.539
T1000151	3443200.02	436775.278	1036.397
T1000152	3443206.59	436767.704	1036.441
T1000153	3443213	436758.421	1036.513
T1000154	3443220.48	436748.464	1036.618
T1000155	3443226.93	436755.088	1036.791
T1000156	3443247.28	436763.526	1036.642
T1000157	3443246.83	436769.559	1036.476
T1000158	3443245.65	436780.256	1036.295
T1000159	3443239.38	436781.738	1036.298
T1000160	3443230.55	436783.613	1036.556
T1000161	3443215.09	436786.496	1036.631
T1000162	3443204.47	436788.649	1036.593
T1000163	3443216.55	436778.482	1036.687
T1000164	3443228.4	436766.623	1036.747
T1000165	3443261.76	436747.131	1037.138
T1000166	3443261.19	436754.016	1037.007
T1000167	3443260.31	436761.259	1036.832
T1000168	3443257.57	436767.612	1036.536
T1000169	3443255.85	436775.62	1036.069
T1000170	3443266.83	436773.5	1035.869
T1000171	3443267.72	436777.491	1035.496
T1000172	3443272.29	436770.24	1036.197
T1000173	3443278.34	436773.357	1035.606
T1000174	3443278.95	436767.336	1036.428
T1000175	3443281.17	436759.885	1037.045
T1000176	3443274.88	436751.307	1037.033

Arroyo Balluco GPS Data

Data collected using Trimble 3100 GPS System
Datum is WGS 84
Coordinates are UTM Grid east and north

Point Name	North (m)	East (m)	Elevation (m)
ROAD0177	3443259.4	436745.078	1036.772
ROAD0178	3443253.86	436749.459	1036.88
ROAD0179	3443257.19	436756.515	1036.508
ROAD0180	3443251.13	436763.428	1036.17
ROAD0181	3443254.31	436770.307	1035.725
ROAD0182	3443249.57	436775.633	1035.289
ROAD0183	3443252.22	436779.477	1035.293
ROAD0184	3443248.68	436780.913	1035.426
T1000185	3443246.32	436783.073	1035.468
T1000186	3443244.79	436781.759	1035.586
T1000187	3443240.23	436785.515	1035.526
T1000188	3443239.42	436783.572	1035.67
T1000189	3443227.38	436786.25	1035.78
T1000190	3443227.75	436788.921	1035.437
T1000191	3443218.95	436788.003	1035.738
T1000192	3443218.69	436790.906	1035.335
T1000193	3443204.55	436790.884	1035.664
T1000194	3443204.09	436793.603	1035.272
T1000195	3443123.84	436825.92	1034.489
T1000196	3443237.12	436826.001	1036.791
hypCenter	3443212.25	436747.219	1032.539
hypCenter	3443205	436755.594	1032.539
hypCenter	3443198.25	436764.344	1032.539
hypCenter	3443192.25	436771.688	1032.539
hypCenter	3443182.5	436780.719	1032.539
hypCenter	3443179.75	436786.75	1032.539
hypCenter	3443177	436792.063	1032.539
hypCenter	3443174	436800.375	1033.164
hypCenter	3443169.75	436806.594	1033.164
hypCenter	3443165.5	436812.125	1033.164
hypCenter	3443160.25	436815.125	1033.789
hypCenter	3443156.25	436815.625	1033.789
hypCenter	3443151.25	436816.406	1033.789
hypCenter	3443143.5	436815.563	1033.789
hypCenter	3443138	436815.125	1033.789
hypCenter	3443128.75	436817.969	1033.789
hypCenter	3443120	436823.719	1033.789
hypCenter	3443114	436830.594	1033.789
hypCenter	3443108	436840.969	1033.789
hypCenter	3443104.75	436847.969	1033.789
hypCenter	3443100.5	436856.219	1033.789
hypCenter	3443094.25	436865.781	1033.789
hypCenter	3443089.25	436874.813	1033.789

Appendix B

Raw EM data

Riverside Electromagnetic Data in MS/m

	Vertical Orientation		Horizontal Orientation				
POINT	Quadraphase	Inphase	Quadraphase	Inphase	North (m)	East (m)	Elev (m)
1	85.625	4.207	52.3	6.84	3503508.692	373900.794	1095.23
2	75.85	4.03	46.7	6.497	3503500.261	373899.526	1095.23
3	89.825	4.277	44.625	6.425	3503492.588	373898.438	1095.22
4	103.7	4.372	44.3	6.385	3503485.907	373897.485	1095.19
5	88	4.165	48.45	6.22	3503479.226	373896.64	1095.13
6	76.3	3.65	40	6.025	3503468.939	373895.489	1095
7	45.35	5.025	33.15	3.607	3503460.699	373896.41	1095.13
8	38.575	3.475	23.525	5.45	3503453.601	373897.928	1095.09
9	24.425	6.097	18.35	2.745	3503451.546	373889.399	1093.68
10	28.35	6.2	21.225	2.06	3503458.276	373889.034	1093.54
11	32.4	6.08	20.6	3.037	3503467.053	373889.295	1093.68
12	36.4	6.102	21.425	2.867	3503475.662	373889.422	1093.81
13	38.875	6.347	27.3	2.912	3503484.378	373890.021	1093.76
14	37.975	6.12	29.925	2.997	3503491.247	373890.871	1094.01
15	38.475	5.855	31.375	2.775	3503500.606	373888.98	1093.83
16	31.25	6.517	21.875	2.565	3503484.94	373885.698	1093.77
17	27.775	5.947	21.375	3.007	3503476.505	373884.253	1093.67
18	25.75	6.37	24.375	2.855	3503467.983	373883.108	1093.63
19	25.675	5.635	16.675	3.032	3503457.36	373882.045	1093.54
20	25.125	6.092	19.75	2.727	3503451.321	373881.844	1093.51
21	28.2	5.645	23.375	3.092	3503450.787	373876.285	1093.53
22	28.575	6.325	18.8	3.085	3503457.22	373875.755	1093.48
23	25.5	6	19.35	3.462	3503468.454	373876.981	1093.57
24	23.775	5.99	19.275	3.17	3503477.252	373877.888	1093.65
25	28	6.177	19.825	2.94	3503486.475	373879.772	1093.66
26	31.8	6.137	29.85	2.802	3503494.99	373882.129	1093.72
27	36.1	5.965	32.325	2.192	3503502.175	373883.861	1093.83
28	28.35	5.707	21.5	3.247	3503506.79	373877.399	1093.99
29	27.8	5.287	22.15	2.615	3503498.104	373871.782	1093.64
30	21.675	5.95	15.75	2.317	3503489.079	373866.165	1093.53
31	22.85	5.405	15.05	2.587	3503479.368	373864.473	1093.48
32	28.55	4.722	27.25	6.297	3503469.916	373863.99	1093.46
33	44.775	7.032	35.375	8.092	3503457.714	373867.232	1093.49
34	29.45	2.877	24.5	5.435	3503449.725	373871.21	1093.54
35	34.65	8.447	21.75	2.905	3503447.031	373864.579	1092.71
36	29.475	6.415	17.925	3.192	3503443.229	373857.176	1092.89
37	44.025	6.077	27.825	4.962	3503440.733	373847.375	1093.02
38	39.05	7.832	22.05	3.797	3503445.736	373843.544	1092.98
39	53.65	12.447	47.55	13.565	3503447.773	373850.329	1092.95
40	55.3	11.955	38.575	7.857	3503451.838	373859.494	1092.71
41	72.5	12.712			3503456.851	373858.64	1092.61
42	47.15	10.437	32.65	5.422	3503456.452	373852.151	1093.06
43	53.925	14.11	20.125	3.437	3503455.85	373844.789	1093.15
44	57.85	17.057	20.5	3.642	3503462.588	373844.159	1092.96
45	90.05	18.905	29.525	6.01	3503466.903	373837.065	1093.01

Riverside Electromagnetic Data in MS/m

	Vertical Orientation		Horizontal Orientation				
POINT	Quadraphase	Inphase	Quadraphase	Inphase	North (m)	East (m)	Elev (m)
46	68.25	19.4	46.225	7.652	3503464.95	373849.273	1092.74
47	94.55	20.477	43.875	10.972	3503465.665	373853.896	1092.58
48	75.95	17.157	48.9	7.802	3503471.883	373848.938	1092.73
49	46.475	10.285	30.925	4.115	3503471.919	373844.148	1092.8
50	45.675	10.842	21.1	4.247	3503473.446	373835.287	1092.99
51	34.85	5.825	29	4.285	3503476.897	373842.038	1092.8
52	32.3	5.38	23.475	2.832	3503481.917	373841.774	1092.72
53	31.925	5.627	26.425	2.962	3503480.766	373837.531	1092.77
54	29.55	5.127	21.475	2.957	3503483.996	373828.899	1093.01
55	25.775	6.712	22.375	3.16	3503490.888	373825.77	1093.01
56	34.025	3.99	22.425	3.12	3503492.579	373834.017	1092.9
57	29.9	2.577	24.025	6.862	3503496.388	373837.812	1093.51
58	37.575	2.405	30.025	4.642	3503499.3	373846.577	1093.06
59	31	5.177	20.975	2.46	3503503.914	373853.258	1092.66
60	35.475	5.445	25.575	2.822	3503508.751	373849.302	1092.67
61	37.725	5.147	35.625	2.71	3503500.412	373839.005	1093.26

Alamo Arroyo Electromagnetic Data in MS/m

	Vertical Orientation		Horizontal Orientation				
Point	Quadraphase	Inphase	Quadraphase	Inphase	North (m)	East (m)	Elev (m)
91	108.4	13.152	78.25	8.117	3464573.48	413694.881	1052.66
92	110.6	13.275	87.125	8.667	3464575.62	413691.834	1052.6
93	130.1	14.422	85.9	8.467	3464578.62	413687.904	1052.56
94	119.5	13.965	86.6	7.537	3464581.39	413684.257	1052.76
95	115.975	12.622	89.625	6.97	3464576.93	413680.408	1052.7
96	131.15	14.082	93.475	8.852	3464574.02	413684.117	1052.3
97	101.95	11.98	84.175	8.917	3464571.11	413686.88	1052.47
98	110.2	13.9	76.675	7.412	3464570.1	413690.854	1052.34
99	111.175	13.09	81.225	7.347	3464567.04	413688.964	1052.11
100	120.175	14.005	94.125	7.94	3464566.16	413683.486	1051.7
101	117.775	13.58	89.925	8.945	3464563.63	413685.471	1051.9
102	127.55	13.592	108.8	9.11	3464561.83	413682.148	1051.71
103	108.675	12.002	82.975	6.66	3464567.45	413676.248	1052.26
104	109.525	12.815	88	7.762	3464573.1	413677.941	1052.42
105	122.65	13.387	104.975	7.75	3464557.71	413683.031	1051.71
106	128.65	13.287	114.925	8.067	3464554.48	413679.747	1051.56
107	132.525	13.625	125.35	7.747	3464551.8	413680.965	1051.5
108	126.9	12.765	95.725	7.667	3464549.4	413682.926	1051.81
109	117.675	12.227	89.3	6.965	3464546.82	413680.155	1051.6
110	140.25	13.14	111.225	8.065	3464548.96	413678.367	1051.33
111	143.125	13.565	124.925	7.735	3464551.02	413677.099	1051.2
112	123.8	11.972	117.9	7.775	3464553.79	413675.14	1052.04
113	134.15	13.017	127.325	8.317	3464548.71	413673.889	1051.23
114	125.35	13.277	99.65	6.305	3464544.74	413676.473	1051.21

Appendix C

Particle Distributions for Each Field Site Investigated

Size Class	RD1 10.15- 9.2	RD1 5.5 -4.7	RD1 3.75 -0.00	RD2 0-5	RD2 5-10	RD2 10-15	RD2 15-19	RD2 19-22	RD2 22-25	RD3 0-4	RD3 4-12	RD4 0-4	RD4 4-8	L1 0-4	L1 4-8	L1 8-12	L2 0-4	L2 4-8	L2 8-12
0.055	0	0	0	0	0	0	0.02	0.01	0.01	0	0	0.03	0.02	0.01	0.02	0.01	0	0	0.02
0.065	0	0	0	0	0	0.01	0.05	0.03	0.02	0	0	0.06	0.03	0.02	0.05	0.02	0.01	0.01	0.05
0.075	0	0	0	0	0	0.02	0.08	0.06	0.04	0	0	0.1	0.06	0.03	0.07	0.03	0.01	0.01	0.08
0.085	0	0.01	0	0	0	0.03	0.12	0.09	0.07	0	0	0.15	0.09	0.05	0.11	0.05	0.02	0.02	0.11
0.1	0	0.01	0	0	0	0.06	0.17	0.15	0.12	0	0	0.2	0.13	0.08	0.15	0.08	0.04	0.04	0.14
0.12	0	0.02	0	0	0	0.09	0.24	0.22	0.19	0	0	0.26	0.18	0.11	0.19	0.11	0.06	0.06	0.18
0.14	0	0.04	0.01	0	0	0.15	0.32	0.32	0.28	0	0	0.33	0.24	0.14	0.24	0.15	0.09	0.09	0.23
0.16	0.01	0.07	0.02	0	0	0.23	0.42	0.45	0.41	0.01	0	0.41	0.32	0.19	0.29	0.19	0.13	0.13	0.27
0.185	0.03	0.11	0.05	0.01	0.01	0.34	0.53	0.61	0.58	0.02	0	0.48	0.4	0.24	0.35	0.24	0.19	0.17	0.32
0.215	0.06	0.16	0.11	0.02	0.02	0.48	0.64	0.79	0.78	0.04	0	0.55	0.48	0.28	0.4	0.29	0.25	0.23	0.36
0.25	0.09	0.22	0.19	0.05	0.06	0.62	0.74	0.98	0.98	0.08	0	0.6	0.54	0.33	0.44	0.34	0.3	0.29	0.39
0.29	0.13	0.26	0.29	0.09	0.1	0.73	0.81	1.13	1.15	0.13	0	0.63	0.58	0.35	0.46	0.37	0.35	0.33	0.41
0.335	0.16	0.28	0.35	0.12	0.13	0.78	0.83	1.18	1.24	0.16	0	0.61	0.57	0.36	0.46	0.38	0.36	0.34	0.41
0.39	0.16	0.28	0.37	0.12	0.14	0.77	0.82	1.16	1.26	0.16	0	0.58	0.54	0.34	0.44	0.37	0.34	0.33	0.39
0.455	0.15	0.27	0.38	0.13	0.14	0.77	0.8	1.17	1.29	0.16	0	0.54	0.5	0.33	0.41	0.35	0.33	0.31	0.37
0.535	0.15	0.25	0.4	0.13	0.14	0.76	0.79	1.17	1.34	0.16	0	0.49	0.45	0.31	0.38	0.34	0.31	0.29	0.35
0.626	0.14	0.23	0.39	0.12	0.13	0.74	0.78	1.16	1.36	0.14	0	0.45	0.4	0.28	0.36	0.32	0.28	0.27	0.32
0.725	0.13	0.22	0.39	0.11	0.12	0.74	0.8	1.18	1.45	0.13	0	0.42	0.36	0.27	0.34	0.3	0.27	0.25	0.31
0.845	0.13	0.22	0.4	0.1	0.12	0.8	0.88	1.28	1.63	0.13	0	0.43	0.37	0.28	0.35	0.31	0.28	0.26	0.32
0.985	0.13	0.23	0.43	0.1	0.12	0.88	0.96	1.41	1.85	0.13	0	0.45	0.38	0.29	0.37	0.33	0.29	0.27	0.34
1.15	0.14	0.25	0.47	0.11	0.13	0.98	1.11	1.57	2.12	0.14	0	0.49	0.4	0.31	0.4	0.35	0.31	0.29	0.36
1.34	0.16	0.28	0.53	0.12	0.14	1.12	1.26	1.77	2.44	0.15	0	0.53	0.43	0.33	0.44	0.38	0.34	0.32	0.4
1.56	0.17	0.31	0.6	0.13	0.16	1.27	1.43	1.99	2.79	0.16	0	0.59	0.47	0.36	0.48	0.42	0.37	0.35	0.43
1.81	0.19	0.34	0.66	0.14	0.16	1.43	1.61	2.22	3.16	0.17	0	0.65	0.52	0.39	0.53	0.46	0.41	0.39	0.48
2.115	0.21	0.38	0.73	0.16	0.18	1.61	1.81	2.45	3.53	0.19	0	0.73	0.57	0.42	0.58	0.51	0.46	0.43	0.53
2.465	0.23	0.43	0.81	0.17	0.2	1.8	2.01	2.68	3.87	0.21	0	0.81	0.63	0.46	0.65	0.56	0.51	0.48	0.59
2.87	0.26	0.48	0.88	0.19	0.22	1.98	2.2	2.88	4.16	0.23	0	0.9	0.71	0.5	0.71	0.62	0.56	0.54	0.65
3.345	0.29	0.53	0.95	0.21	0.24	2.16	2.4	3.05	4.38	0.26	0	1.01	0.79	0.55	0.79	0.68	0.63	0.6	0.72
3.895	0.33	0.58	1	0.23	0.27	2.33	2.59	3.18	4.52	0.29	0	1.13	0.89	0.6	0.86	0.75	0.69	0.66	0.78
4.535	0.37	0.64	1.05	0.26	0.31	2.48	2.76	3.25	4.56	0.33	0	1.25	0.98	0.65	0.94	0.81	0.76	0.73	0.85
5.285	0.4	0.69	1.07	0.29	0.34	2.59	2.91	3.25	4.48	0.36	0	1.36	1.1	0.7	1.02	0.86	0.83	0.79	0.92
6.16	0.43	0.73	1.05	0.31	0.36	2.67	3.02	3.17	4.28	0.4	0	1.5	1.21	0.74	1.09	0.94	0.9	0.86	0.98
7.175	0.45	0.77	1.01	0.33	0.38	2.7	3.1	3.01	3.98	0.43	0	1.62	1.32	0.78	1.16	1.01	0.96	0.92	1.04
8.36	0.46	0.79	0.93	0.34	0.39	2.68	3.12	2.79	3.59	0.45	0	1.74	1.43	0.82	1.23	1.07	1.02	0.98	1.1
9.74	0.46	0.8	0.84	0.34	0.37	2.63	3.1	2.53	3.14	0.47	0	1.87	1.58	0.85	1.3	1.13	1.06	1.04	1.15
11.345	0.45	0.8	0.73	0.32	0.35	2.56	3.03	2.24	2.66	0.49	0	2.01	1.73	0.9	1.38	1.21	1.15	1.12	1.21
13.215	0.46	0.81	0.64	0.31	0.32	2.47	2.93	1.95	2.18	0.51	0	2.18	1.96	0.98	1.48	1.3	1.24	1.2	1.28
15.395	0.48	0.83	0.57	0.31	0.3	2.39	2.8	1.69	1.73	0.54	0	2.39	2.27	1.11	1.61	1.43	1.36	1.31	1.37
17.94	0.53	0.87	0.52	0.32	0.3	2.32	2.67	1.48	1.32	0.58	0.25	2.66	2.68	1.3	1.77	1.58	1.53	1.44	1.48
20.9	0.6	0.93	0.51	0.34	0.3	2.27	2.55	1.31	0.94	0.63	0.27	2.97	3.19	1.56	1.96	1.79	1.74	1.6	1.61
24.345	0.69	1.01	0.5	0.38	0.31	2.23	2.45	1.19	0.74	0.66	0.28	3.32	3.78	1.92	2.17	2.04	2	1.79	1.77
30.865	0.77	1.09	0.5	0.41	0.3	2.2	2.36	1.12	0.64	0.66	0.25	3.68	4.41	2.36	2.44	2.34	2.31	2.02	1.95
33.045	0.83	1.16	0.46	0.42	0.28	2.15	2.29	1.09	0.6	0.62	0.19	4.01	5.01	2.84	2.64	2.67	2.67	2.28	2.16
38.495	0.83	1.21	0.4	0.39	0.22	2.05	2.21	1.07	0.57	0.52	0.12	4.27	5.51	3.36	2.86	3.02	3.06	2.58	2.4
44.85	0.73	1.21	0.3	0.31	0.16	1.91	2.13	1.07	0.52	0.38	0.07	4.41	5.66	3.67	3.07	3.37	3.48	2.92	2.68
52.25	0.57	1.19	0.19	0.21	0.09	1.72	2.01	1.08	0.42	0.24	0.03	4.4	5.98	4.33	3.27	3.7	3.91	3.31	3
60.87	0.4	1.17	0.06	0.12	0.06	1.52	1.87	1.11	0.27	0.15	0	4.25	5.93	4.72	3.46	4.03	4.34	3.76	3.37
70.915	0.16	1.22	0.07	0.08	0.08	1.35	1.71	1.18	0.07	0.06	0.02	3.97	5.76	5.03	3.67	4.34	4.75	4.25	3.8
82.615	0.21	1.41	0.16	0.12	0.2	1.29	1.54	1.29	0	0.12	0.08	3.59	5.1	5.26	3.91	4.63	5.14	4.78	4.28
96.245	0.43	1.8	0.39	0.27	0.46	1.33	1.4	1.46	0	0.31	0.26	3.17	4.36	5.43	4.19	4.92	5.49	5.31	4.79
112.13	0.9	2.44	0.87	0.59	0.96	1.54	1.34	1.86	0	0.72	0.71	2.72	3.61	5.55	4.51	5.18	5.79	5.82	5.3
130.63	1.75	3.36	1.78	1.21	1.94	1.9	1.37	2.11	0	1.53	1.66	2.37	2.92	5.63	4.85	5.43	6.09	6.3	5.81
152.18	3.14	4.55	3.35	2.36	3.69	2.35	1.46	2.62	0	3.06	3.38	2.14	2.34	5.69	5.2	5.86	6.01	6.72	6.3
177.29	5.3	5.96	5.88	4.43	6.6	3.05	1.6	3.1	0.09	5.74	6.09	2.04	1.89	5.5	5.34	5.57	5.66	6.6	6.37
206.54	8.34	7.46	9.42	7.79	10.57	3.65	1.76	3.43	0.47	9.74	9.73	2.04	1.55	5.1	5.21	5.21	5.02	6.09	6.09
240.62	11.94	8.93	13.52	12.13	14.66	4.01	1.9	3.6	1.19	14.35	13.84	2.1	1.29	4.48	4.79	4.6	4.17	5.22	5.43
280.32	15.22	10.18	14.42	15.63	17.23	3.89	2.01	3.23	2.11	17.86	17.65	2.16	1.07	3.58	4.11	3.8	3.22	4.12	4.48
326.57	14.47	9.62	12.37	16.73	14.93	3.59	2.06	2.63	2.97	15.58	16.87	2.14	0.86	2.81	3.28	2.93	2.32	2.99	3.36
380.45	11.47	8.08	8.82	13.36	10.94	2.92	2.03	1.82	3.38	10.91	13.51	2.02	0.65	1.98	2.44	2.1	1.58	1.96	2.23
443.23	7.58	5.99	5.21	9.15	6.87	2.09	1.87	1.01	3.03	6.24	8.93	1.77	0.43	1.26	1.6	1.36	1.03	1.13	1.1
516.36	4.3	3.94	2	5.68	2.79	1.26	1.54	0.2	2.05	2.12	4.71	1.42	0.22	0.57	0.77	0.63	0.65	0.3	0
601.56	1.41	1.89	0	2.2	0	0.43	1.08	0	0.86	0	1.1	1.01	0.01	0	0	0	0.41	0	0
700.82	0	0	0	0	0	0	0.62	0	0.14	0	0	0.6	0	0	0	0	0.17	0	0
816.45	0	0	0	0	0	0	0.16	0	0	0	0	0.19	0	0	0	0	0	0	0
855	2.6	3.16	0	1.61	1.02	0	0	0	0	0.92	0.39	5	7.6	2.49	3.06	3.01	3.07	2.93	3.62
1580	4.55	9.54	0	5.2	0	0	0	0	0	2.18	2.21	14.43	27.36	5.23	6.4	6.45	5.81	4.86	6.21
3080	3.29	2.87	0	4.47	0	0	0	0	0	1.5	0.3	23.29	38.42	2.17	6.66	5.4	4.58	4.29	7.28
5080	0.36	0	0	0.13	0	0	0	0	0	0	0.31	17	2.82	0.51	11.84	5.74	1.5	0.31	0.42
mean size	420.7390719	354.2305199	298.3823609	464.1077152	289.4314498	112.3317809	95.6164768	87.0064225	82.8397991	325.4915549	344.547393	1703.174065	1140.699579	248.0701103	953.2808226	610.1412997	373.9504133	311.4630847	409.9739942

AA1 9-14	AA2 0-3	AA2 3-7	AA2 7-12	AA3 0-4	AA3 4-8	AA3 8-12	AA3 12-16	AA4 0-4	AA4 4-8	AA4 8-12	AA4 12-16	AA4 16-20	AA4 20-24	AA4 24-28	AA4 28-32	AA4 32-36
0	0	0	0	0	0	0	0	0	0	0	0	0	0	0	0	0
0	0.01	0	0	0	0	0	0	0	0	0	0	0	0	0	0	0
0	0.01	0.01	0	0	0	0	0	0	0	0	0	0	0	0	0	0
0	0.02	0.01	0	0	0	0	0	0	0	0	0	0	0	0	0	0
0	0.03	0.02	0	0.01	0	0	0	0	0	0	0	0	0	0	0	0
0.01	0.04	0.03	0	0.01	0	0	0	0	0	0	0	0	0	0	0	0
0.01	0.07	0.04	0.01	0.02	0	0	0	0	0	0	0	0	0	0	0	0
0.02	0.1	0.06	0.02	0.03	0	0	0	0	0	0	0	0	0	0	0	0
0.04	0.14	0.09	0.03	0.04	0	0	0	0.01	0	0	0.01	0.01	0.01	0.01	0.01	0.01
0.06	0.19	0.12	0.04	0.05	0	0	0	0.02	0.01	0.01	0.01	0.02	0.02	0.01	0.01	0.01
0.09	0.23	0.16	0.06	0.06	0	0	0	0.04	0.02	0.02	0.02	0.03	0.03	0.03	0.03	0.03
0.1	0.27	0.18	0.08	0.07	0	0	0	0.06	0.04	0.04	0.04	0.04	0.04	0.04	0.04	0.04
0.11	0.28	0.19	0.09	0.07	0	0	0	0.08	0.06	0.05	0.05	0.05	0.05	0.05	0.05	0.05
0.11	0.26	0.19	0.09	0.07	0	0	0	0.08	0.06	0.06	0.05	0.05	0.05	0.05	0.06	0.05
0.11	0.27	0.19	0.09	0.07	0	0	0	0.08	0.07	0.06	0.05	0.06	0.05	0.06	0.06	0.06
0.11	0.26	0.18	0.09	0.07	0	0	0	0.08	0.07	0.06	0.05	0.06	0.05	0.06	0.06	0.06
0.1	0.25	0.17	0.08	0.06	0	0	0	0.08	0.06	0.06	0.05	0.05	0.05	0.05	0.06	0.05
0.1	0.25	0.17	0.08	0.06	0	0	0	0.07	0.06	0.05	0.05	0.05	0.05	0.05	0.05	0.05
0.11	0.26	0.18	0.08	0.06	0	0	0	0.06	0.05	0.05	0.04	0.05	0.04	0.04	0.05	0.04
0.11	0.26	0.19	0.09	0.07	0	0	0	0.06	0.05	0.05	0.04	0.04	0.04	0.04	0.04	0.04
0.12	0.31	0.2	0.09	0.07	0	0	0	0.06	0.05	0.05	0.04	0.04	0.04	0.04	0.04	0.04
0.13	0.34	0.22	0.1	0.07	0	0	0	0.07	0.05	0.04	0.04	0.04	0.04	0.04	0.04	0.04
0.14	0.39	0.24	0.11	0.07	0	0	0	0.07	0.05	0.04	0.03	0.03	0.03	0.03	0.03	0.03
0.16	0.43	0.26	0.12	0.07	0	0	0	0.07	0.05	0.04	0.03	0.03	0.03	0.02	0.03	0.03
0.17	0.48	0.29	0.14	0.07	0	0	0	0.07	0.05	0.03	0.02	0.02	0.03	0.02	0.02	0.03
0.19	0.54	0.32	0.15	0.08	0	0	0	0.07	0.05	0.03	0.02	0.02	0.03	0.02	0.02	0.03
0.21	0.6	0.36	0.17	0.08	0	0	0	0.07	0.05	0.03	0.02	0.02	0.03	0.02	0.02	0.03
0.23	0.66	0.39	0.19	0.09	0	0	0	0.08	0.05	0.04	0.03	0.03	0.03	0.03	0.03	0.03
0.26	0.71	0.42	0.22	0.1	0	0	0	0.09	0.07	0.05	0.04	0.04	0.04	0.04	0.04	0.04
0.28	0.76	0.45	0.24	0.11	0	0	0	0.11	0.08	0.06	0.05	0.05	0.05	0.05	0.05	0.05
0.3	0.81	0.48	0.26	0.12	0	0	0	0.12	0.09	0.07	0.06	0.05	0.06	0.06	0.06	0.07
0.32	0.84	0.49	0.27	0.12	0	0	0	0.13	0.1	0.08	0.07	0.06	0.07	0.06	0.06	0.08
0.33	0.86	0.49	0.27	0.12	0	0	0	0.13	0.1	0.08	0.07	0.05	0.07	0.06	0.06	0.08
0.33	0.86	0.49	0.27	0.1	0	0	0	0.12	0.09	0.08	0.06	0.04	0.06	0.04	0.04	0.07
0.32	0.86	0.47	0.25	0.08	0	0	0	0.1	0.07	0.06	0.04	0.03	0.05	0.03	0.03	0.05
0.29	0.86	0.45	0.22	0.06	0	0	0	0.07	0.05	0.04	0.02	0.02	0.03	0.02	0.02	0.03
0.25	0.86	0.42	0.19	0.05	0	0	0	0.05	0.03	0.03	0	0.02	0.02	0.02	0.02	0
0.22	0.88	0.4	0.16	0.04	0	0	0	0.04	0.03	0.03	0	0.03	0.03	0.03	0.03	0
0.18	0.92	0.38	0.13	0.05	0	0	0	0.05	0.05	0.03	0	0.04	0.04	0.05	0.05	0
0.15	1	0.38	0.11	0.07	0	0	0	0.07	0.06	0.04	0	0.05	0.05	0.06	0.05	0
0.13	1.11	0.4	0.09	0.1	0	0	0	0.08	0.06	0.05	0	0.06	0.06	0.06	0.06	0
0.12	1.26	0.45	0.09	0.12	0	0	0	0.08	0.06	0.05	0	0.06	0.07	0.06	0.05	0
0.11	1.46	0.52	0.09	0.12	0	0	0	0.07	0.05	0.05	0	0.05	0.06	0.05	0.05	0
0.1	1.69	0.63	0.09	0.11	0	0	0	0.06	0.04	0.04	0	0.04	0.05	0.04	0.03	0
0.08	1.94	0.77	0.09	0.09	0	0	0	0.04	0.03	0.03	0	0.03	0.04	0.03	0.02	0
0.06	2.19	0.96	0.07	0.06	0	0	0	0.02	0.02	0.02	0	0.02	0.02	0.02	0.02	0
0.04	2.43	1.19	0.06	0.01	0	0	0	0.02	0.02	0.02	0.02	0.02	0.02	0.02	0.02	0.02
0.04	2.64	1.47	0.05	0.02	0.06	0.06	0	0.03	0.04	0.03	0.05	0.06	0.04	0.08	0.07	0.05
0.08	2.62	1.63	0.06	0.07	0.16	0.17	0.03	0.1	0.11	0.1	0.16	0.19	0.12	0.22	0.22	0.16
0.22	2.96	2.26	0.19	0.23	0.44	0.46	0.11	0.26	0.3	0.27	0.43	0.51	0.32	0.57	0.56	0.42
0.51	3.14	2.79	0.43	0.65	1.03	1.05	0.35	0.68	0.74	0.67	1.02	1.18	0.78	1.3	1.3	1
1.06	3.32	3.42	0.87	1.53	2.09	2.08	0.93	1.54	1.72	1.55	2.22	2.51	1.7	2.78	2.82	2.23
1.93	3.54	4.14	1.69	3.13	3.76	3.88	2.07	3.24	3.64	3.23	4.39	4.85	3.38	5.37	5.53	4.46
3.19	3.83	4.93	2.67	5.6	6.1	5.88	4.06	6.25	6.99	6.13	7.76	8.36	6.05	9.17	9.57	7.98
4.85	4.19	5.75	4.12	8.78	8.85	8.48	6.95	10.61	11.52	10.14	11.86	12.35	9.5	13.29	13.92	12.26
6.81	4.63	6.58	5.9	12.11	11.56	11.1	10.5	15.34	15.69	14.23	15.54	15.6	12.94	16.33	16.91	16.06
8.85	5.14	7.38	7.62	14.78	13.68	13.24	14.06	18.52	17.16	16.53	17.63	17.25	15.2	17.29	17.52	17.88
10.8	5.7	8.15	9.71	16.57	15.12	14.77	17.11	16.48	16.11	16.54	15.28	14.7	16.03	13.91	13.66	15.06
12.61	6.14	8.39	11.5	14.18	13.43	13.34	15.99	12.42	12.04	12.87	11.5	10.9	13.45	9.83	9.31	11.05
12.63	6.23	8.14	13.07	10.26	10.43	10.57	12.65	8.07	7.97	8.68	7.51	6.98	9.73	6.05	5.47	7.06
11.51	5.85	7.36	12.72	6.3	7.43	7.8	8.63	3.72	3.9	5.34	3.53	3.07	6.28	2.28	1.62	3.08
9.18	4.96	6.05	11.09	2.73	4.43	5.04	4.91	0	0	1.99	0	0	2.82	0	0	0
6.28	3.63	4.33	8.35	0	1.43	2.27	1.64	0	0	0	0	0	0	0	0	0
3.07	1.96	2.3	4.63	0	0	0	0	0	0	0	0	0	0	0	0	0
6.26	3.7	4.37	6.94	2.2	0.24	0.35	0.4	0.32	0.24	0.44	0.1	0.07	0.21	0.06	0.04	0.05
7.27	5.12	6.47	5.77	0.52	0.1	0.18	0.13	0.22	0.14	0.11	0.06	0.03	0.06	0.03	0.04	0.05
5.1	8.01	7.38	3.41	0.12	0.06	0.07	0.05	0.07	0.15	0.07	0.15	0.02	0.06	0.02	0.03	0.03
6.4	9.56	13.29	3.58	0.03	0	0.12	0	0.6	0.04	0.03	0.17	0	0	0	0	0
28.5600685	1009.186002	1239.908166	773.1141333	350.1483256	348.78247	363.0330965	370.625436	388.0387683	310.9337926	325.9897496	313.3991555	294.791758	329.799016	286.8332875	282.5577386	297.380018

DISTRIBUTION

External

Richard Langford
Department of Geological Sciences
University of Texas at El Paso
El Paso, TX 79968-0555

US Army Corps of Engineers
Coastal and Hydraulics Laboratory
CEWES-CC-C
3909 Halls Ferry Rd
Vicksburg, MS 39180
Attn: Joseph Gailani

Rong Kuo
International Boundary and Water Commission
4171 N. Mesa C-310
El Paso, TX 79902

Manuel Rubio, Jr.
International Boundary and Water Commission
4171 N. Mesa C-310
El Paso, TX 79902-1441

Paul Tashjian
Department of the Interior
US FISH AND WILDLIFE SERVICE
P.O. Box 1306
Albuquerque, NM 87103-1306

Thanos N. Papanicolaou
Washington State University
PO Box 642910
Pullman, WA 99164-2910

Jerry Wall
U.S. Department of the Interior
Bureau of Land Management
435 Montano N.E.
Albuquerque, NM 87107

Craig Jones
Woods Hole Group
1167 Oddstad Dr.
Redwood City, CA 94063

U.S. Army Corps of Engineers
Coastal and Hydraulics Laboratory
CEWES-CC-D
3909 Halls Ferry Rd
Vicksburg, MS 39180
Attn: Jarrel Smith

John R. Gray
U.S. Department of the Interior
U.S. Geological Survey
12201 Sunrise Valley Drive
415 National Center
Reston, VA 20192

John W. Longworth
P.O. Box 25102
Santa Fe, NM 87504-5102

Pravi Shrestha
HydroQual, Inc.
One Lethbridge Plaza
Mahwah, NJ 07430

Rodrick D. Lentz
U.S. Department of Agriculture
3793 N. 3600 E.
Kimberly, ID 83341-5076

Christopher J. McArthur, P.E.
U.S. EPA Region 4
Wetlands, Coastal & NonPoint
Source Branch
61 Forsyth Street, S.W.
Atlanta, GA 30303

Kirk Ziegler
Quantitative Environmental Analysis, LLC
305 West Grand Avenue
Montvale, NJ 07645

Joseph V. DePinto
Senior Scientist
Limno-Tech, Inc.
501 Avis Drive
Ann Arbor, MI 48108

Wilbert J. Lick
Dept. of Mechanical
& Environmental Engineering
University of California, Santa Barbara
Santa Barbara, CA 93106-5070

Gary Scott
U.S. Dept. of Energy
P.O. Box 3090, GSA 220
Carlsbad, NM 88221-3090

Internal

MS	Org.	
0701	6100	W. Cieslak
0701	6100	P. Davies
0735	6115	D. Thomas
0735	6115	E. Webb
0755	6251	M. Hightower
0771	6800	D.R. Anderson
1395	6820	P.E. Shoemaker
1395	6822	F.D. Hansen
1395	6822	R. Jepsen
1395	6822	J. Roberts
1395	6820	F.C. Allan (6)
9018	8495-1	Central Technical Files
0899	9616	Technical Library (2)
0612	9612	Review and Approval Desk for DOE/OSTI